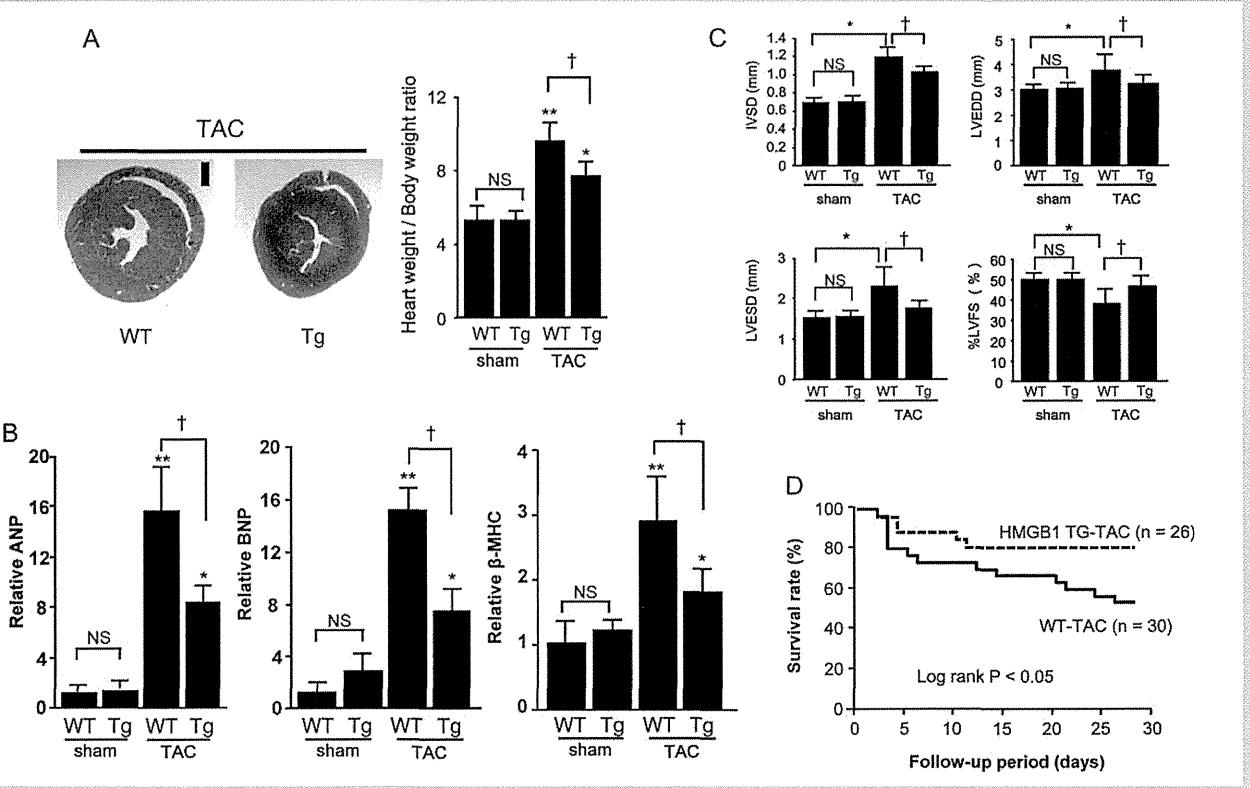


**Figure 5** Suppression of DNA damage induced by pressure overload in HMGB-1 Tg mice. (*A*) Left-ventricular transverse sections in WT and HMGB1-Tg mice at 4 weeks after TAC, and heart weight: body ratios in TAC or sham-operated mice. Data are mean ± SEM from eight mice for each group. $^{*}P < 0.05$ and $^{**}P < 0.01$ vs. sham-operated mice of the same strain; $^{\dagger}P < 0.05$ vs. TAC-operated Tg mice. (*B*) Quantitative analyses of ANP, BNP, and β-MHC gene expression in WT and HMGB1-Tg mice at 4 weeks after TAC. Data are mean ± SEM from eight mice for each group. $^{*}P < 0.05$ and $^{**}P < 0.01$ vs. sham-operated mice of the same strain; $^{\dagger}P < 0.05$ vs. TAC-operated Tg mice. (*C*) Data showing echocardiographic measurements in WT and HMGB1-Tg mice at 4 weeks after TAC or sham surgery. IVS, interventricular wall thickness; LVEDD, left-ventricular end-diastolic dimension; LVESD, left-ventricular end-systolic dimension; %LVFS, left-ventricular fractional shortening. Data are mean ± SEM from eight mice for each group. $^{*}P < 0.05$ vs. sham-operated WT mice; $^{\dagger}P < 0.05$ vs. TAC-operated WT mice. (*D*) Survival curves in WT and HMGB1-Tg mice after TAC.

from the nucleus have been reported.[17] Prior studies have reported that post-translational modification of HMGB1 including acetylation in cultured cells modifies the binding of HMGB1 to DNA and its extranuclear localization.[17,34,35] Hyperacetylation of HMGB1 induced by lipopolysaccharide and hydrogen peroxide triggers its translocation into the cytoplasm.[17,36] In the present study, stimulation of cardiomyocytes with ET-1 or Ang II and pressure overload in mice induced the acetylation and translocation of nuclear HMGB1. To the best of our knowledge, this is the first report of HMGB1 acetylation and translocation from the nucleus in cardiomyocytes.

Whether extracellular HMGB1 acts as a cardioprotective factor is the subject of controversy, and the effect of nuclear HMGB1 under hypertrophic stimulation is also poorly understood. We showed that the expression of foetal genes induced by ET-1 was inhibited by HMGB1 overexpression. In addition, we showed that pressure overload-induced foetal gene expression is attenuated in HMGB1-Tg mice compared with WT mice. Oxidative stress induced by pressure overload contributes to cardiac DNA damage and DNA repair/synthesis in failing hearts with systolic dysfunction.[37] Therefore, DNA damage is thought to be a key pathogenic factor in ventricular dysfunction.[14] A recent study showed the involvement of intracellular HMGB1 in protecting against DNA damage in the brain and in neurons.[20,21] Nuclear HMGB1 was recruited to sites of cellular oxidative DNA base damage, and cell-based experiments and biochemical data suggested that HMGB1 plays a role in base excision repair.[15,20,21] In the present study, 8-OHdG induction after TAC was significantly attenuated in HMGB1-Tg mice compared with WT mice. Taken together, these findings indicate that nuclear HMGB1 might prevent DNA damage during pressure overload, as seen in the decrease in cardiac dysfunction in HMBG1-Tg mice. HMGB1 translocation induced by hypertrophic stimulation might cause DNA damage, increasing the severity of cardiac hypertrophy, affecting foetal gene expression, and causing cardiac dysfunction.

There are several limitations in this study. In the present study, we showed that maintenance of HMGB1-TG in cardiomyocyte and the heart prevent cardiac dysfunction after pressure overload, however, we did not show the direct link between reduced HMGB1 in the heart and cardiac dysfunction *in vivo* study. To confirm this point, we might need to evaluate cardiac function in cardiac-specific HMGB1 knockout mice in the future study. However, we demonstrated that intranuclear HMGB1 was reduced in failing heart, and HMGB1 silencing promoted foetal gene expressions. Therefore, the findings of this study suggest a novel approach to the investigation of the pathogenesis of heart

failure, and nuclear HMGB1 may be a potential novel therapeutic target for the prevention of heart failure.

# 5. Conclusions

We demonstrated that nuclear HMGB1 was decreased in association with human heart failure and preserved amounts of nuclear HMGB1 could prevent cardiac hypertrophy and improve survival in a pressure overload heart failure model.

# Supplementary material

Supplementary material is available at *Cardiovascular Research* online.

## Acknowledgements

We thank Ms Emiko Nishidate and Ms Miyuki Tsuda for their excellent technical assistance.

**Conflict of interest:** none declared.

## Funding

This work was supported in part by a grant-in-aid for Scientific Research (Nos. 21590923 and 24659380 to I.K., 25860580 to A.F., and 23790830 to T.S.) from the Ministry of Education, Science, Sports, and Culture, Japan, a grant-in-aid from the 21st Global Century Center of Excellence (COE) program of the Japan Society for the Promotion of Science to I.K. T.S. was supported by the Japan Heart Foundation Research Grant. The funders had no role in study design, data collection and analysis, decision to publish, or preparation of the manuscript.

## References

1. Jessup M, Brozena S. Heart failure. *N Engl J Med* 2003;**348**:2007–2018.
2. McMurray JJ, Pfeffer MA. Heart failure. *Lancet* 2005;**365**:1877–1889.
3. Roger VL, Weston SA, Redfield MM, Hellermann-Homan JP, Killian J, Yawn BP *et al.* Trends in heart failure incidence and survival in a community-based population. *JAMA* 2004;**292**:344–350.
4. Rame JE, Ramilo M, Spencer N, Blewett C, Mehta SK, Dries DL *et al.* Development of a depressed left ventricular ejection fraction in patients with left ventricular hypertrophy and a normal ejection fraction. *Am J Cardiol* 2004;**93**:234–237.
5. Nightingale K, Dimitrov S, Reeves R, Wolffe AP. Evidence for a shared structural role for HMG1 and linker histones B4 and H1 in organizing chromatin. *EMBO J* 1996;**15**: 548–561.
6. Lange SS, Mitchell DL, Vasquez KM. High mobility group protein B1 enhances DNA repair and chromatin modification after DNA damage. *Proc Natl Acad Sci USA* 2008; **105**:10320–10325.
7. Calogero S, Grassi F, Aguzzi A, Voigtlander T, Ferrier P, Ferrari S *et al.* The lack of chromosomal protein Hmg1 does not disrupt cell growth but causes lethal hypoglycaemia in newborn mice. *Nat Genet* 1999;**22**:276–280.
8. Scaffidi P, Misteli T, Bianchi ME. Release of chromatin protein HMGB1 by necrotic cells triggers inflammation. *Nature* 2002;**418**:191–195.
9. Yang H, Hreggvidsdottir HS, Palmblad K, Wang H, Ochani M, Li J *et al.* A critical cysteine is required for HMGB1 binding to Toll-like receptor 4 and activation of macrophage cytokine release. *Proc Natl Acad Sci USA* 2010;**107**:11942–11947.
10. Lotze MT, Tracey KJ. High-mobility group box 1 protein (HMGB1): nuclear weapon in the immune arsenal. *Nat Rev Immunol* 2005;**5**:331–342.
11. Germani A, Limana F, Capogrossi MC. Pivotal advances: high-mobility group box 1 protein–a cytokine with a role in cardiac repair. *J Leukoc Biol* 2007;**81**:41–45.
12. Kitahara T, Takeishi Y, Harada M, Niizeki T, Suzuki S, Sasaki T *et al.* High-mobility group box 1 restores cardiac function after myocardial infarction in transgenic mice. *Cardiovasc Res* 2008;**80**:40–46.
13. Andrassy M, Volz HC, Riedle N, Gitsioudis G, Seidel C, Laohachewin D *et al.* HMGB1 as a predictor of infarct transmurality and functional recovery in patients with myocardial infarction. *J Intern Med* 2011;**270**:245–253.
14. Suzuki S, Shishido T, Ishino M, Katoh S, Sasaki T, Nishiyama S *et al.* 8-Hydroxy-2′-deoxyguanosine is a prognostic mediator for cardiac event. *Eur J Clin Invest* 2011;**41**:759–766.
15. Prasad R, Liu Y, Deterding LJ, Poltoratsky VP, Kedar PS, Horton JK *et al.* HMGB1 is a cofactor in mammalian base excision repair. *Mol Cell* 2007;**27**:829–841.
16. Evankovich J, Cho SW, Zhang R, Cardinal J, Dhupar R, Zhang L *et al.* High mobility group box 1 release from hepatocytes during ischemia and reperfusion injury is mediated by decreased histone deacetylase activity. *J Biol Chem* 2010;**285**:39888–39897.
17. Bonaldi T, Talamo F, Scaffidi P, Ferrera D, Porto A, Bachi A *et al.* Monocytic cells hyperacetylate chromatin protein HMGB1 to redirect it towards secretion. *EMBO J* 2003;**22**: 5551–5560.
18. Tang D, Kang R, Livesey KM, Kroemer G, Billiar TR, Van Houten B *et al.* High-mobility group box 1 is essential for mitochondrial quality control. *Cell Metab* 2011;**13**:701–711.
19. El Gazzar M, Yoza BK, Chen X, Garcia BA, Young NL, McCall CE. Chromatin-specific remodeling by HMGB1 and linker histone H1 silences proinflammatory genes during endotoxin tolerance. *Mol Cell Biol* 2009;**29**:1959–1971.
20. Enokido Y, Yoshitake A, Ito H, Okazawa H. Age-dependent change of HMGB1 and DNA double-strand break accumulation in mouse brain. *Biochem Biophys Res Commun* 2008; **376**:128–133.
21. Qi ML, Tagawa K, Enokido Y, Yoshimura N, Wada Y, Watase K *et al.* Proteome analysis of soluble nuclear proteins reveals that HMGB1/2 suppress genotoxic stress in polyglutamine diseases. *Nat Cell Biol* 2007;**9**:402–414.
22. Kuwahara K, Saito Y, Ogawa E, Takahashi N, Nakagawa Y, Naruse Y *et al.* The neuron-restrictive silencer element-neuron-restrictive silencer factor system regulates basal and endothelin 1-inducible atrial natriuretic peptide gene expression in ventricular myocytes. *Mol Cell Biol* 2001;**21**:2085–2097.
23. Kuwahara K, Saito Y, Takano M, Arai Y, Yasuno S, Nakagawa Y *et al.* NRSF regulates the fetal cardiac gene program and maintains normal cardiac structure and function. *EMBO J* 2003;**22**:6310–6321.
24. Shishido T, Woo CH, Ding B, McClain C, Molina CA, Yan C *et al.* Effects of MEK5/ERK5 association on small ubiquitin-related modification of ERK5: implications for diabetic ventricular dysfunction after myocardial infarction. *Circ Res* 2008;**102**:1416–1425.
25. Le NT, Takei Y, Shishido T, Woo CH, Chang E, Heo KS *et al.* p90RSK targets the ERK5-CHIP ubiquitin E3 ligase activity in diabetic hearts and promotes cardiac apoptosis and dysfunction. *Circ Res* 2012;**110**:536–550.
26. Woo CH, Massett MP, Shishido T, Itoh S, Ding B, McClain C *et al.* ERK5 activation inhibits inflammatory responses via peroxisome proliferator-activated receptor delta (PPARdelta) stimulation. *J Biol Chem* 2006;**281**:32164–32174.
27. Woo CH, Le NT, Shishido T, Chang E, Lee H, Heo KS *et al.* Novel role of C terminus of Hsc70-interacting protein (CHIP) ubiquitin ligase on inhibiting cardiac apoptosis and dysfunction via regulating ERK5-mediated degradation of inducible cAMP early repressor. *FASEB J* 2010;**24**:4917–4928.
28. Pallier C, Scaffidi P, Chopineau-Proust S, Agresti A, Nordmann P, Bianchi ME *et al.* Association of chromatin proteins high mobility group box (HMGB) 1 and HMGB2 with mitotic chromosomes. *Mol Biol Cell* 2003;**14**:3414–3426.
29. Murai K, Naruse Y, Shaul Y, Agata Y, Mori N. Direct interaction of NRSF with TBP: chromatin reorganization and core promoter repression for neuron-specific gene transcription. *Nucleic Acids Res* 2004;**32**:3180–3189.
30. Andrassy M, Volz HC, Igwe JC, Funke B, Eichberger SN, Kaya Z *et al.* High-mobility group box-1 in ischemia-reperfusion injury of the heart. *Circulation* 2008;**117**:3216–3226.
31. Limana F, Germani A, Zacheo A, Kajstura J, Di Carlo A, Borsellino G *et al.* Exogenous high-mobility group box 1 protein induces myocardial regeneration after infarction via enhanced cardiac C-kit+ cell proliferation and differentiation. *Circ Res* 2005; **97**:e73–e83.
32. El Gazzar M. HMGB1 modulates inflammatory responses in LPS-activated macrophages. *Inflamm Res* 2007;**56**:162–167.
33. Treutiger CJ, Mullins GE, Johansson AS, Rouhiainen A, Rauvala HM, Erlandsson-Harris H *et al.* High mobility group 1 B-box mediates activation of human endothelium. *J Intern Med* 2003;**254**:375–385.
34. Assenberg R, Webb M, Connolly E, Stott K, Watson M, Hobbs J *et al.* A critical role in structure-specific DNA binding for the acetylatable lysine residues in HMGB1. *Biochem J* 2008;**411**:553–561.
35. Pasheva E, Sarov M, Bidjekov K, Ugrinova I, Sarg B, Lindner H *et al.* In vitro acetylation of HMGB-1 and -2 proteins by CBP: the role of the acidic tail. *Biochemistry* 2004; **43**:2935–2940.
36. Ugrinova I, Pashev IG, Pasheva EA. Nucleosome binding properties and Co-remodeling activities of native and in vivo acetylated HMGB-1 and HMGB-2 proteins. *Biochemistry* 2009;**48**:6502–6507.
37. Siggens L, Figg N, Bennett M, Foo R. Nutrient deprivation regulates DNA damage repair in cardiomyocytes via loss of the base-excision repair enzyme OGG1. *FASEB J* 2012; **26**:2117–2124.

OPEN ACCESS Freely available online

PLOS ONE

# Direct Immunochemiluminescent Assay for proBNP and Total BNP in Human Plasma proBNP and Total BNP Levels in Normal and Heart Failure

**Toshio Nishikimi[1]*, Hiroyuki Okamoto[2], Masahiro Nakamura[2], Naoko Ogawa[2], Kazukiyo Horii[2], Kiyoshi Nagata[2], Yasuaki Nakagawa[1], Hideyuki Kinoshita[1], Chinatsu Yamada[1], Kazuhiro Nakao[1], Takeya Minami[1], Yoshihiro Kuwabara[1], Koichiro Kuwahara[1], Izuru Masuda[3], Kenji Kangawa[4], Naoto Minamino[5], Kazuwa Nakao[1]**

**1** Department of Medicine and Clinical Science, Kyoto University Graduate School of Medicine, Kyoto, Japan, **2** Diagnostics Division, Shionogi & Co., Ltd, Osaka, Japan, **3** Takeda Hospital Medial Examination Center, Kyoto, Japan, **4** Department of Biochemistry National Cerebral and Cardiovascular Center Research Institute, Osaka, Japan, **5** Department of Molecular Pharmacology, National Cerebral and Cardiovascular Center Research Institute, Osaka, Japan

## Abstract

***Background:*** Recent studies have shown that in addition to brain (or B-type) natriuretic peptide (BNP) and the N-terminal proBNP fragment, levels of intact proBNP are also increased in heart failure. Moreover, present BNP immunoassays also measure proBNP, as the anti-BNP antibody cross-reacts with proBNP. It is important to know the exact levels of proBNP in heart failure, because elevation of the low-activity proBNP may be associated with the development of heart failure.

***Methodology/Principal Findings:*** We therefore established a two-step immunochemiluminescent assay for total BNP (BNP+proBNP) and proBNP using monoclonal antibodies and glycosylated proBNP as a standard. The assay enables measurement of plasma total BNP and proBNP within only 7 h, without prior extraction of the plasma. The detection limit was 0.4 pmol/L for a 50-μl plasma sample. Within-run CVs ranged from 5.2%–8.0% in proBNP assay and from 7.0%–8.4% in total BNP assay, and between-run CVs ranged from 5.3–7.4% in proBNP assay and from 2.9%–9.5% in total BNP assay, respectively. The dilution curves for plasma samples showed good linearity (correlation coefficients = 0.998–1.00), and analytical recovery was 90–101%. The mean total BNP and proBNP in plasma from 116 healthy subjects were 1.4±1.2 pM and 1.0±0.7 pM, respectively, and were 80±129 pM and 42±70 pM in 32 heart failure patients. Plasma proBNP levels significantly correlate with age in normal subjects.

***Conclusions/Significance:*** Our immunochemiluminescent assay is sufficiently rapid and precise for routine determination of total BNP and proBNP in human plasma.

**Citation:** Nishikimi T, Okamoto H, Nakamura M, Ogawa N, Horii K, et al. (2013) Direct Immunochemiluminescent Assay for proBNP and Total BNP in Human Plasma proBNP and Total BNP Levels in Normal and Heart Failure. PLoS ONE 8(1): e53233. doi:10.1371/journal.pone.0053233

**Editor:** German E. Gonzalez, University of Buenos Aires, Cardiovascular Pathophysiology Institute, Argentina

**Received** July 10, 2012; **Accepted** November 26, 2012; **Published** January 24, 2013



**Funding:** This study was supported in part by Scientific Research Grants-in-Aid 20590837 and 23591041 from the Ministry of Education, Culture, Sports, Science and Technology of Japan (to T. Nishikimi); a grant (AS 232Z01302F) from the Japan Science and Technology Agency (to T. Nishikimi); a grant from the Suzuken Memorial Foundation (to T. Nishikimi); and the Intramural Research Fund of National Cerebral and Cardiovascular Center of Japan (to N. Minamino). The funders had no role in study design, data collection and analysis, decision to publish, or preparation of the manuscript.

**Competing Interests:** Hiroyuki Okamoto, Masahiro Nakamura, Naoko Ogawa, Kazukiyo Horii and Kiyoshi Nagata are employed by Shionogi& Co., Ltd. Shionogi Company previously developed the BNP kit and they may develop a new assay kit like a proBNP in the future. There are no further patents, products in development or marketed products to declare. This does not alter the authors' adherence to all the PLOS ONE policies on sharing data and materials.

* E-mail: nishikim@kuhp.kyoto-u.ac.jp

## Introduction

Brain (also known as B-type) natriuretic peptide (BNP) has been used as a biomarker of heart failure for more than a decade [1]. Indeed, guidelines for the treatment of heart failure recommend measurement BNP before making a diagnosis [2,3]. During the process by which BNP is secreted from cardiac myocytes, its 108-amino acid precursor, proBNP, is cleaved to form the 32-amino acid peptide BNP and the 76-amino acid peptide N-terminal proBNP fragment (NT-proBNP) [4]. Recent studies have shown that in addition to BNP and the NT-proBNP, levels of uncleaved proBNP are also considerably increased in plasma of patients with heart failure [5,6,7]. This is noteworthy in part because the immunoassay system currently being used to measure BNP levels also detects proBNP, as the anti-BNP antibody cross-reacts with proBNP. Consequently, the present assay system actually measures not the active BNP level, but the total BNP (BNP+proBNP) level [8].

It is important to know the proBNP level and/or proBNP/total BNP ratio in heart failure, because proBNP has much less ability to induce cGMP production (about 13–17%) than BNP, and higher levels of the low-activity proBNP may be associated with the development of heart failure [7]. Consistent with that idea, we recently used the combination of gel-filtration and a fluorescent immunoenzyme assay with BNP extracted from plasma to show

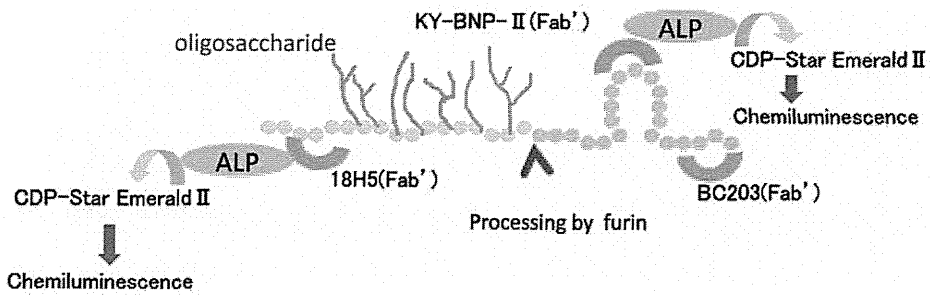


**Figure 1. Schematic diagram of the total BNP and proBNP assay systems.** BC203(Fab') is a common capture antibody in both systems. KY-BNP-II(Fab') is the detection antibody for the total BNP assay, and 18H5(Fab') is the detection antibody for the proBNP assay. ALP: Alkaline phosphatase; CDP-Star EmeraldII (Chemiluminescent Substrate): Disodium 2-chloro-5-(4-methoxy-spiro{1,2-dioxetane-3,2′-(5′-chloro)-tricyclo [3,3,1,13,7]decan}-4-yl)-1-phenyl phosphate.
doi:10.1371/journal.pone.0053233.g001

that although proBNP/total BNP ratios vary widely in heart failure, they are higher in cases of ventricular overload than in atrial overload [6]. Unfortunately, the method used in that study requires a great deal of time and effort, and extraction of the peptide from plasma may cause underestimation of the proBNP levels due to its high adsorptive property [9].

To overcome those shortcomings, we developed a sensitive method to more quickly and easily measure levels of proBNP and total BNP. Our idea was to make a sandwich immunoassay using a common capture antibody recognizing the C-terminal region of both BNP and proBNP and detection antibodies that recognize different epitopes: the N-terminal region of proBNP and the ring structure of BNP (Figure 1). Using this approach, we were able to develop a sensitive immunochemiluminescent assay for proBNP and total BNP in plasma. Here, we report on the assay's performance and its use to compare plasma levels of total BNP and proBNP in healthy subjects and patients with heart failure. In addition, we measured NT-proBNP and compared it with total BNP and proBNP.

## Materials and Methods

All patients provided written informed consent for all blood sample analyses, and the protocol was approved by the Ethical Committee of Kyoto University Graduate School of Medicine. Sample analyses were also conducted in accordance with the policies and procedures of the Institutional Review Board for the use of human subjects in research at the Diagnostics Division of Shionogi & Co., Ltd.

### Peptides and Reagents

Glycosylated proBNP and recombinant proBNP were purchased from Hytest Ltd. (Turk, Finland). The protein content was determined by amino acid analysis. BNP was from Peptide Institute, Inc. (Osaka, Japan). EZ-Link-sulfo-NHS-biotinylation kits were from Pierce (Rockford, IL). Sulfo-HMCS (N-(8-maleimidocapryloxy) sulfosuccinimide) was from Dojindo (Kumamoto, Japan). CDP/E (Disodium 2-chloro-5-(4-methoxy-spiro{1,2-dioxetane-3,2′-(5′-chloro)-tricyclo [3,3,1,13,7]decan}-4-yl)-1-phenyl phosphate) was from Applied Biosystems (Foster City, CA).

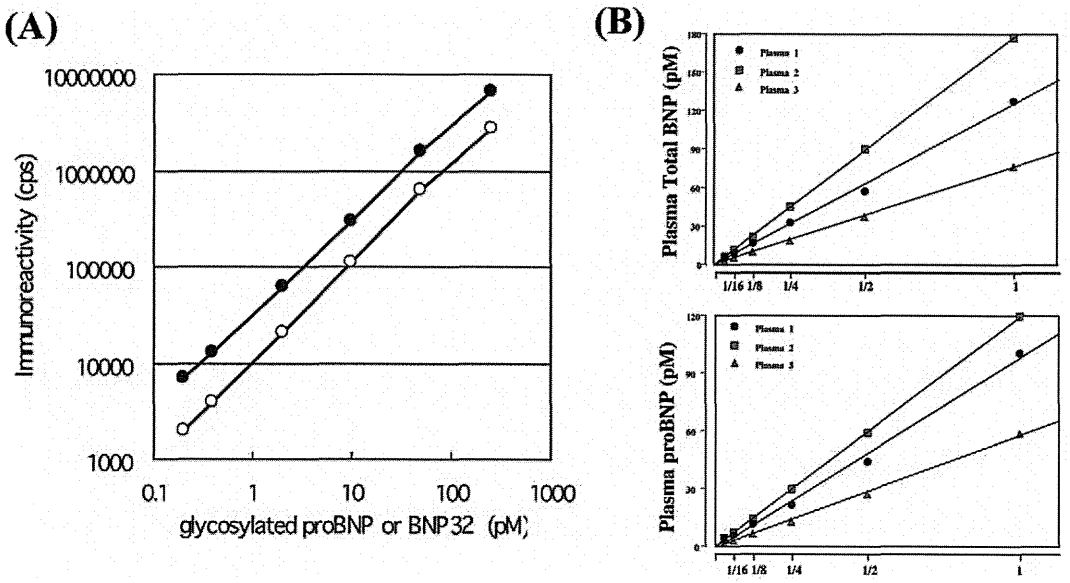


**Figure 2. Standard curves for the proBNP (open circle) and total BNP (closed circle) assays (A). Plasma dilution curves (B).** Three plasma samples collected from three heart failure patients were serially diluted with buffer.
doi:10.1371/journal.pone.0053233.g002

**Table 1.** Recovery of standard glycosylated proBNP and BNP added to human plasma.

| Added peptide concentration, pmol/L | Recovery, % | Recovery, % |
|---|---|---|
| | proBNP assay system | total BNP assay system |
| 2.0 | 90 | 85 |
| 25.0 | 101 | 97 |
| 100.0 | 95 | 95 |

doi:10.1371/journal.pone.0053233.t001

## Antibodies

The monoclonal antibodies BC203 (IgG1, k) and KY-BNP-II (IgG1, k) were developed by Shionogi & Co., Ltd [10]. BC203 and KY-BNP-II recognize the C-terminal region and the ring region of BNP, respectively. The monoclonal antibody 18H5 was purchased from Hytest Ltd. 18H5 recognizes a region (a.a. 13–20) of proBNP. In the proBNP assay, the combination of BC203 (capture) and 18H5 (detection) was used because 18H5 is not affected by glycosylation [11]. In the total BNP assay, the combination of BC203 (capture) and KY-BNP-II (detection) was used because KY-BNP-II recognizes nearly all bioactive BNPs (Figure 1).

## Preparation of BC203 coated immunoassay plates

BC203, which was the capture antibody in both assays, was biotinylated using an EZ-Link-sulfo-NHS-biotinylation kit according to the manufacturer's instructions. The biotinylated BC203 (0.2 mg/well in 100 mL PBS) was added to streptavidin-coated plates and incubated for 18 h at 4°C. After washing with a saline containing 0.01 g/dL Tween 20 and 0.05 g/dL sodium azide (Wash Buffer), the BC203 coated immunoassay plates were dried in a desiccator.

## Preparation of 18H5 (Fab')-ALP and KY-BNP-II (Fab')-ALP

The 18H5 and KY-BNP-II mAbs (IgG) were digested with pepsin (IgG/pepsin = 1/0.05) for 4 h at 37°C in 100 mM citrate buffer (pH 4.0) containing 100 mM NaCl. Thereafter, Fab' solution was prepared by reduction with 10 mM 2-mercaptoethylamine in 0.1 M phosphate buffer (pH 6.0) containing 5 mM EDTA using the standard method [12]. Alkaline phosphatase from calf intestine (ALP; 2.0 mg or 14.2 nmol; Kikkoman, Chiba, Japan) in 0.475 mL 0.1 M Tris-HCl buffer (pH 7.0) containing 1 mM MgCl2 and 0.1 mM ZnCl2 was mixed with 31 mg (71 nmol) of Sulfo-HMCS in 0.05 mL of water for 1.5 h on ice, after which the HMCS-activated ALP was purified on a PD-10 column (GE Healthcare, Chalfont St. Giles, UK). Aliquots of HMCS-activated ALP solution (0.96 mg in 0.192 mL) were each added to 0.441 mg of the Fab' in 0.15 mL of 0.1 M phosphate buffer (pH 6.0) containing 5 mM EDTA and mixed for 16 h at 4°C. Unlabeled Fab' antibody was removed using a TSKgel 3000SWxl column. The purified 18H5 (Fab')-ALP and KY-BNP-II (Fab')-ALP were then diluted with a StabilZyme AP (BioFX Lab.) and stored at 4°C until use.

## Sandwich 2-step Chemiluminescent Enzyme Immunoassay

After the BC203 coated immunoassay plates were washed with a wash buffer, 50 mL of test sample or calibrator and 50 mL of Assay Buffer (0.05 M Tris-HCl buffer (pH 7.4), 1 g/dL BSA, 0.01 g/dL Tween80, 1 mM MgCl2, 0.1 mM ZnCl2, 1000K IU/mL Aprotinin, 0.1 mg/mL mouse gamma globulin, 0.9 g/dL NaCl) were added to the wells. The plates were then incubated for 3 h at 25°C. After washing with wash buffer, 100 mL of detection antibodies (18H5 (Fab')-ALP, 100 ng/ml; KY-BNP-II (Fab')-ALP, 416 ng/ml) were added to the wells. The plates were then incubated for 1 h at 25°C, followed by washing with wash buffer and addition of substrate (CDP/E) solution. The chemiluminescence from each well was then measured using a plate reader (Wallac 1420 Arvo sx, Perkin Elmer, Inc., MA).

## Study Patients

We collected blood samples from heart failure patients (18 men and 14 women; age range, 34–84 years, mean age, 65±11 years) hospitalized at Kyoto University Hospital. The primary causes of the heart failure were ischemic heart disease (n = 8), cardiomyopathy (n = 8), valvular heart disease (n = 7), pulmonary hypertension (n = 7) and others (n = 2), which were diagnosed from the medical history, physical examination and chest radiographic, electrocar-

**Table 2.** Effects of dilution on recovery rates with the proBNP and total BNP assay systems.

| Dilution magnitude | proBNP assay system | | total BNP assay system | |
|---|---|---|---|---|
| | Measured, pmol/L | Recovery, % | Measured, pmol/L | Recovery, % |
| 1 | 94 | - | 95 | - |
| 2 | 105 | 112 | 101 | 107 |
| 5 | 96 | 102 | 104 | 109 |
| 10 | 92 | 98 | 92 | 97 |
| 20 | 97 | 103 | 93 | 98 |
| 50 | 99 | 105 | 97 | 103 |
| 100 | 87 | 92 | 95 | 100 |

doi:10.1371/journal.pone.0053233.t002

**Table 3.** Intra- and Inter-assay precision of the proBNP assay systems.

| | Added proBNP concentration pmol/L | Measured concentration pmol/L | | CV | Bias |
|---|---|---|---|---|---|
| | | Mean | S.D. | % | % |
| Intra-assay (n = 5) | 2.0 | 2.0 | 0.2 | 8.0 | 2.0 |
| | 25 | 25 | 1.3 | 5.2 | 0.0 |
| | 100 | 101 | 5.5 | 5.4 | 1.0 |
| Inter-assay (n = 15) | 2.0 | 1.9 | 0.1 | 5.3 | −5.8 |
| | 25 | 23 | 1.7 | 7.4 | −8.0 |
| | 100 | 96 | 6.1 | 6.4 | −4.0 |

doi:10.1371/journal.pone.0053233.t003

diographic, echocardiographic and/or cardiac catheterization findings. Patients with symptomatic heart failure were under medication, including angiotensin-converting-enzyme inhibitors/angiotensin-receptor blockers, digitalis and diuretics. The New York Heart Association (NYHA) functional classes were class I–II (n = 19) and class III–IV (n = 13). Healthy subjects (61 men and 54 women; age range, 30–78 years, mean age, 50±10 years) were selected based on their normal physical, laboratory, chest radiographic, electrocardiographic and echocardiographic findings, and their BNP levels.

## Plasma samples

Blood samples were drawn into plastic syringes and quickly transferred to chilled tubes containing EDTA (1.5 mg/mL, blood) and aprotinin (500 U/mL blood) and centrifuged at 1600× g for 20 min at 4°C. The obtained plasma samples were stored at −80°C until assayed.

## Assay of plasma NT-proBNP levels

Plasma levels of NT-proBNP were measured using Elecsys proBNP II assay system (Roche Diagnostics, Basel, Switzerland).

## Gel filtration chromatography

Plasma samples were extracted using Sep-Pak C18 cartridges (Waters, Milford, MA, USA) as previously described [6]. The eluate was lyophilized and dissolved in 30% acetonitrile containing 0.1% TFA. The resultant solution (300 ml) was separated by gel filtration HPLC on a Superdex 75 10/300 GL columns (10×300 mm×2, GE Healthcare) in the same buffer at a flow rate of 0.4 mL/min. The column effluent was fractionated every minute into polypropylene tubes containing bovine serum albumin (100 mg) and each fraction was analyzed using the total BNP and proBNP assay systems. Because recent studies have shown that glycosylated proBNP with a MW of about 30 K circulates in the plasma [7], we examined the gel filtration positions at which commercial recombinant proBNP and glycosylated proBNP, and synthetic BNP were eluted to determine which is the major molecular form of BNP in human plasma.

## Deglycosylation enzyme treatment

We further analyzed the immunoreactive proBNP levels to determine whether immunoreactive proBNP in plasma is glycosylated. Eluate lyophilized after extraction on a Sep-Pak C18 column was dissolved in phosphate buffer and incubated with or without a cocktail of deglycosylation enzymes for 24 h at 37°C, as previously described [13]. The enzyme cocktail included O-glycosidase (Roche Diagnostic) and neuraminidase (Roche Diagnostics) at final concentrations of 4.25 and 42.5 mU/mL, respectively. These two enzymes were essential for the deglycosylation, and the enzyme concentrations and incubation period were selected based on the results of preliminary and previously reported studies [11,13,14]. We then lyophilized the sample again and dissolved it in 30% acetonitrile containing 0.1% TFA, after which it was subjected to gel-filtration HPLC as described above.

## Statistical Analysis

All values are expressed as means ± SD. The statistical significance of differences between 2 groups was evaluated using Fisher's exact test or unpaired Student's t test, as appropriate. Variables were compared among three groups using one-way analysis of variance followed by Bonferroni's multiple comparison

**Table 4.** Intra- and Inter-assay precision of the total BNP systems.

| | Added BNP concentration pmol/L | Measured concentration pmol/L | | CV | Bias |
|---|---|---|---|---|---|
| | | Mean | S.D. | % | % |
| Intra-assay (n = 5) | 2.0 | 2.3 | 0.2 | 7.0 | 15.0 |
| | 25 | 25 | 2.1 | 8.4 | 1.0 |
| | 100 | 99 | 7.1 | 7.2 | −0.7 |
| Inter-assay (n = 15) | 2.0 | 2.1 | 0.2 | 9.5 | 5.0 |
| | 25 | 24 | 1.7 | 2.9 | −4.0 |
| | 100 | 100 | 1.9 | 1.9 | 0.0 |

doi:10.1371/journal.pone.0053233.t004

**Table 5.** Cross-reactivity between proBNP and BNP.

| Added peptide concentration, pmol/L | Added peptide concentration, pmol/L | Measured peptide concentration, pmol/L | Measured peptide concentration, pmol/L |
|---|---|---|---|
| proBNP | BNP | proBNP assay | total BNP assay |
| 50 | 50 | 58 | 114 |
| 100 | 10 | 113 | 119 |
| 10 | 100 | 8 | 113 |

doi:10.1371/journal.pone.0053233.t005

test. Correlation coefficients were calculated using linear regression analysis. Values of $P<0.05$ were considered significant.

## Results

### Standard curve, recovery and precision

Figure 2 shows typical standard curves for the proBNP and total BNP assay systems. The lower detection limits were 0.04 pmol/L (proBNP) and 0.02 pmol/L (total BNP). At these levels the mean value (n = 8 each) of the chemiluminescence intensity (cps) was more than twice that at 0 pmol/L ($P<0.05$). The working range (coefficient of variation (CV)<15%) of both assays was 0.2–250 pmol/L in total BNP and 0.4–250 pmol/L in proBNP, respectively.

Table 1 shows the recovery of standard proBNP and BNP, which was estimated from the levels of glycosylated proBNP or BNP added to clinically available plasma (endogenous total BNP = 0.3 pmol/L and proBNP = 0.2 pmol/L). In the proBNP assay system, using glycosylated proBNP as a standard, the recovery ranged from 90–101%. In the total BNP assay system, using BNP as the standard the recovery ranged from 85–97%. The effect of diluting plasma samples containing 100 pmol/L glycosylated proBNP or BNP is shown in Table 2. At every dilution level, the recovery rate was good. We also investigated the effects of dilution on plasma levels of total BNP and proBNP in three heart failure patients. As shown in Figure 2B, the calculated total BNP and proBNP values varied linearly with dilution (correlation coefficients = 0.998–1.00).

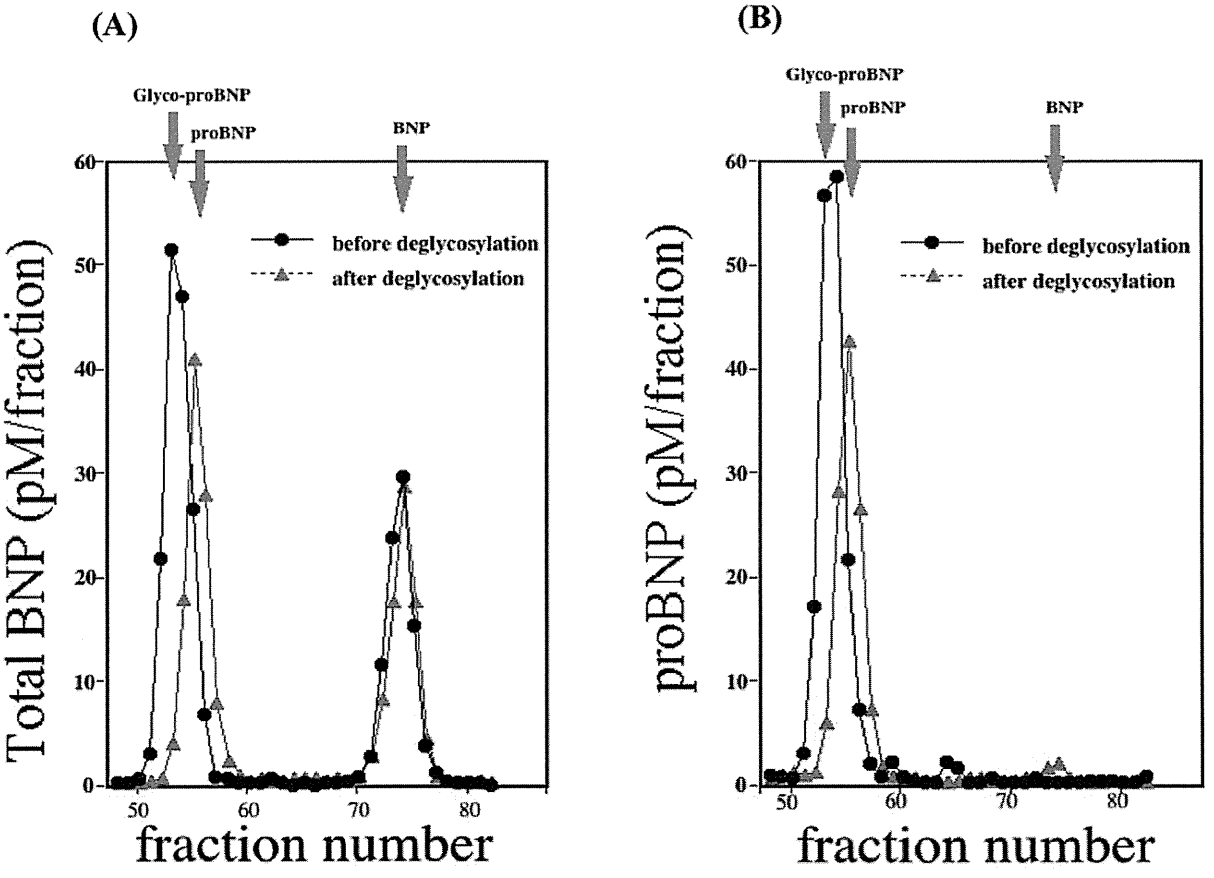


**Figure 3. Gel filtration analysis of total BNP (A) and proBNP (B) in plasma from a heart failure patient.** Fractions were assayed using the total BNP (A) and proBNP (B) systems. The elution points for glycosylated proBNP, proBNP and BNP are indicated by red arrows. Black and red lines respectively show gel filtration analyses of total BNP (A) and proBNP (B) in the same plasma sample before and after deglycosylation.
doi:10.1371/journal.pone.0053233.g003

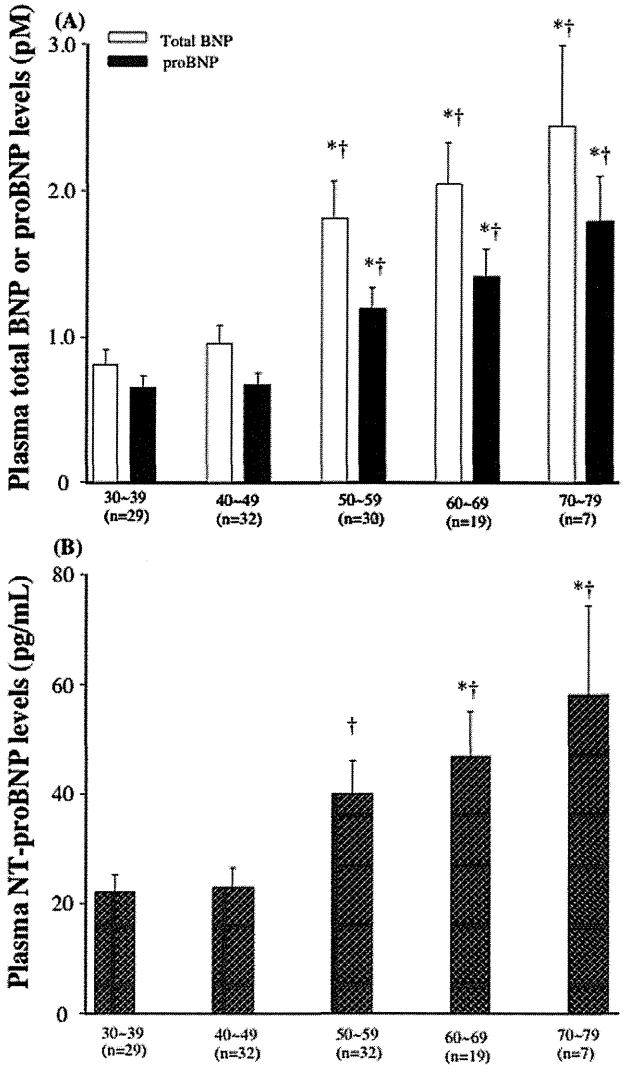


**Figure 4. Plasma Levels of total BNP, proBNP, and NT-proBNP in different age groups.** Bar graph showing the total BNP, proBNP (A) and NT-proBNP levels (B). Values are means ± SE., *P<0.05 vs total BNP, proBNP, and NT-proBNP in 30~39, †P<0.05 vs total BNP, proBNP, and NT-proBNP in 40~49.
doi:10.1371/journal.pone.0053233.g004

When we then assessed the intra- and inter-assay precision using plasma spiked with glycosylated proBNP or BNP, we found that the intra-assay CV ranged from 5.2%–8.0% in proBNP assay and from 7.0%–8.4% in total BNP assay, while inter-assay CV ranged from 5.3–7.4% in proBNP assay and from 1.9%–9.5% in total BNP assay, respectively (Table 3, 4).

### Specificity and sensitivity

We next examined the cross-reactivity between proBNP and BNP. As shown in Table 5, the presence of BNP did not affect the values measured with the proBNP assay system. Moreover, the values measured with the total BNP assay system were the sum of the BNP and proBNP even at different compositions of these two peptides. Thus, the total BNP assay recognized both BNP and proBNP with the same efficiency and sensitivity. Likewise, the proBNP and total BNP assay systems recognized proBNP with the same efficiency and sensitivity.

### Gel-filtration chromatography before and after deglycosylation procedure

Figure 3-A shows two immunoreactive BNP peaks detected using the total BNP assay with HPLC fractions. The first peak appeared in fractions 52–55 and the second peak in fractions 72–75. With the same sample, one immunoreactive BNP peak was detected by the proBNP assay (Figure 3-B); the position of that peak was completely consistent with the proBNP peak obtained with the total BNP assay. When subjected to gel filtration HPLC, recombinant proBNP, glycosylated proBNP and BNP were eluted mainly in fractions 53, 56 and 74, respectively. Treating the same plasma sample with an enzyme cocktail catalyzing deglycosylation shifted the first peak to fraction 54–56, which is consistent with the proBNP peak. From these results, we conclude that total BNP assay evaluates the sum of the glycosylated proBNP plus BNP, while proBNP assay detects glycosylated proBNP. The proBNP was not detected in a significant level with either assay system.

### Plasma concentrations of proBNP, total BNP, and NT-proBNP in healthy subjects and heart failure patients

Plasma total BNP, proBNP and NT-proBNP levels in different age groups were shown in Figure 4-A, B. Plasma total BNP, proBNP and NT-proBNP levels appeared to increase according to the age. The older age groups (more than 50) had higher total BNP, proBNP and NT-proBNP levels than younger age groups (less than 50); however, there were no statistical differences in NT-proBNP between 30~39 and 50~59. In addition, there were significant positive relationships between plasma total BNP ($r = 0.467$, $p<0.001$), proBNP ($r = 0.491$, $p<0.001$) and NT-proBNP ($r = 0.376$, $p<0.001$) levels and age (Figure 5-A, B, C).

The mean total BNP and proBNP in plasma from 116 healthy subjects were $1.4\pm1.2$ pM and $1.0\pm0.7$ pM, respectively (Figure 6-A). Female had higher total BNP than male (total BNP: $1.7\pm1.3$ vs $1.1\pm1.1$, $P<0.05$; proBNP: $1.1\pm0.8$ vs $0.8\pm0.6$ pM, $P = 0.11$) (Figure 6-C). proBNP/total BNP ratio was lower in female than that in male. NT-proBNP was also higher in female than those in male (Figure 6-E). The total BNP and proBNP levels were markedly elevated in heart failure patients, and the magnitude of the increase reflected the severity of the patients' condition as observed in NT-proBNP (Figure 6-A, B).

## Discussion

Plasma levels of the cardiac hormone BNP increase in proportion to the severity of heart failure. Indeed, plasma BNP levels are used as a biomarker of heart failure, and the guidelines in many countries recommend that BNP be used as a diagnostic indicator of acute and chronic heart failure [1–3]. The stimuli that increase cardiac BNP production include pressure overload, volume overload and ischemia, as well as various cytokines and neurohumoral factors [15]. In response to these stimuli, BNP mRNA expression is rapidly upregulated. Following translation of the protein, the signal peptide is removed to produce proBNP, which is then cleaved into BNP and the NT-proBNP fragment during secretion [15]. It is noteworthy that BNP and proBNP could not be distinguished from one another in earlier BNP assay systems because the anti-BNP antibodies cross-reacted with proBNP. We therefore endeavored to develop a new assay system that would enable separate measurement of BNP and proBNP. Recent studies have shown that levels of uncleaved proBNP are increased in heart failure to a greater degree than BNP [5–7,16]. Using a combination of gel filtration and an immunoenzyme fluorescent assay for BNP, we previously found that proBNP levels are increased in heart failure and that the proBNP/total BNP

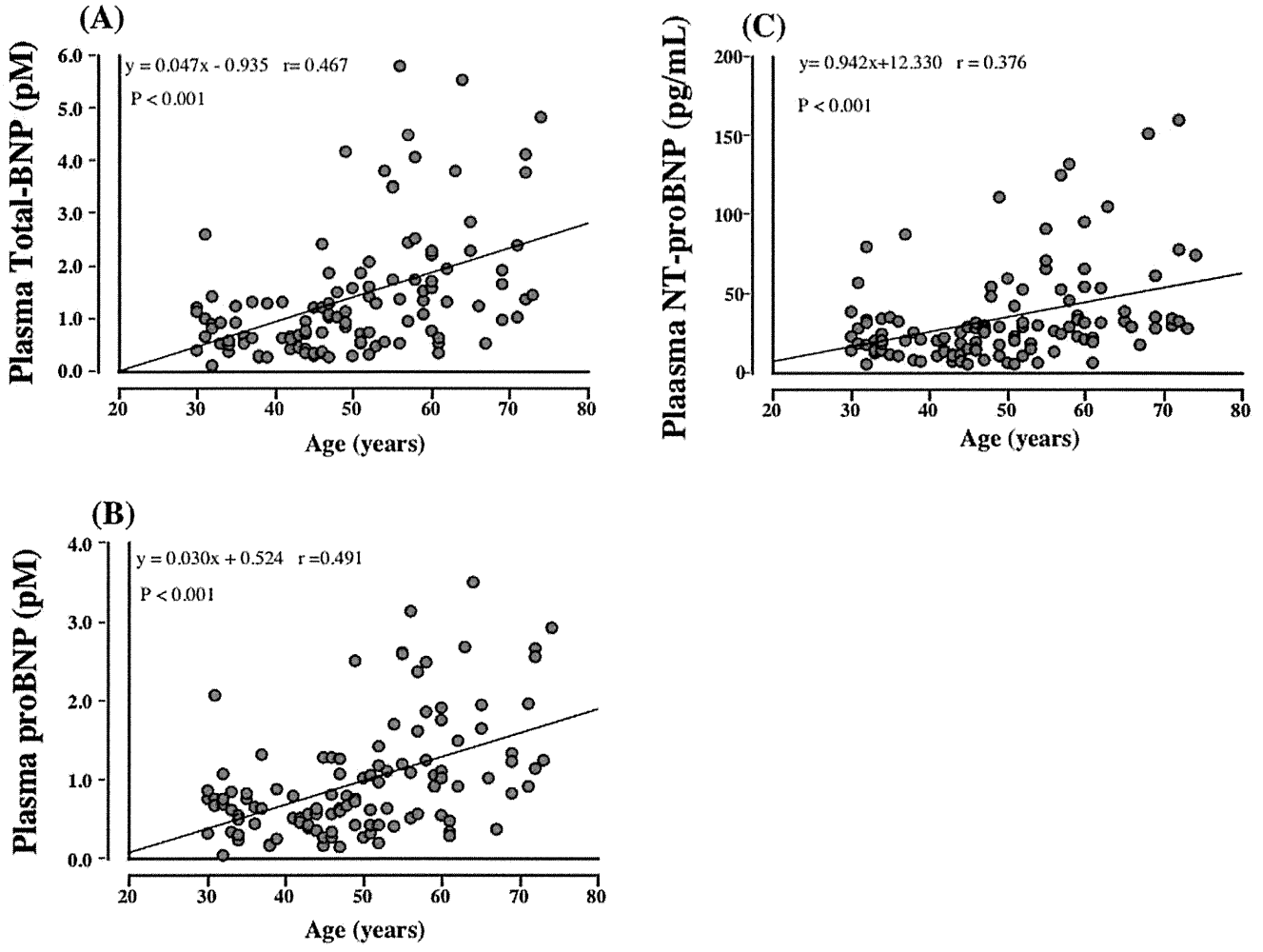


**Figure 5. The relationships between total BNP (A), proBNP (B), and NT-proBNP (C) and age.**
doi:10.1371/journal.pone.0053233.g005

ratios are higher in heart failure patients with ventricular overload than those with atrial overload [6]. Although this protocol provides useful information, the methodology is time-consuming and impractical for routine assays in clinical laboratories. In addition, recovery of proBNP may be diminished by both extraction and the gel filtration steps [9,16]. To overcome these problems, we developed new direct immunochemiluminescent assays for proBNP and total BNP.

We used two monoclonal antibodies, BC203 and 18H5, to assay proBNP. BC203 recognizes an epitope in the C-terminal of proBNP, while 18H5 recognizes an epitope in the N-terminal. Recent studies showed that proBNP has seven sites suitable for *O*-linked oligosaccharide attachment (Ser36, Thr37, Thr44, Thr48, Thr53, Ser58 and Thr71) within the N-terminal portion of the peptide [14]. Because the *O*-linked oligosaccharide attachments almost completely inhibit the binding of the antibody to the peptide [17], we selected 18H5, which recognizes the N-terminal of proBNP (a.a. 13–20) in a region not subject to glycosylation (Figure 1). To assay total BNP, we used the monoclonal antibodies BC203 and KY-BNP-II, as previously reported [10]. In both assays, BC203 served as the capture antibody. Importantly, because the affinity of 18H5 for the N-terminal portion is similar to the affinity of KY-BNP-II for the ring structure, we are able to calculate the proBNP/total BNP ratio. In addition, our new assays are less time-consuming and more sensitive and accurate than earlier ones, and the lower detection limits for total BNP (0.02 pmol/L) and proBNP (0.04 pmol/L) enabled us to measure plasma proBNP levels in nearly all the healthy subjects tested.

We used gel-filtration on two tandemly connected Superdex 75 columns to determine the molecular mass of plasma proBNP. As shown in Figure 3-A,B, a single peak of proBNP was obtained in both the total BNP and proBNP assay systems. The elution points are consistent with that of glycosylated proBNP, but not deglycosylated proBNP, and deglycosylation treatment significantly shifted the peak rightward (Figure 3-A,B) to an elution point consistent with proBNP. The peak immunoreactivity of proBNP after deglycosylation was slightly smaller than before treatment, suggesting the recovery rate of proBNP after gel-filtration is lower than that of glycosylated proBNP, which is consistent with proBNP being more adsorptive than glycosylated proBNP. Our findings are also consistent with previous Western blot analyses showing that plasma levels of glycosylated proBNP are elevated and no substantial level of proBNP is detected in severe heart failure [7]. Taken together, these results suggest that the major molecular form of proBNP in the plasma of patients with heart failure is the glycosylated form.

ProBNP is also the important molecular form of BNP in the plasma of healthy subjects. When we previously used gel-filtration

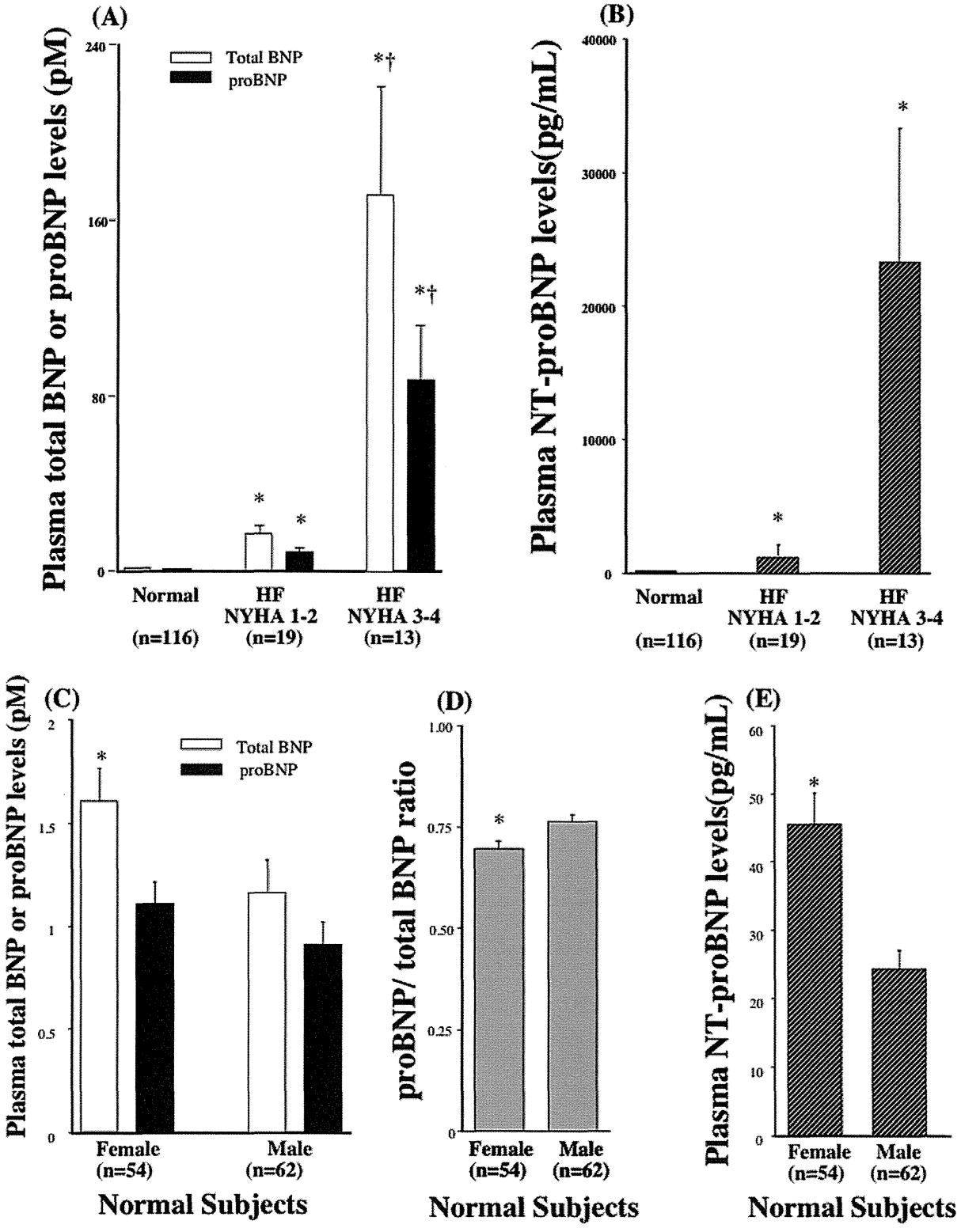


**Figure 6. Plasma Levels of proBNP, total BNP, and NT-proBNP in normal and heart failure.** Bar graph showing the total BNP, proBNP (A) and NT-proBNP (B) levels in healthy subjects and heart failure patients with NYHA classes 1–2 and 3–4. *P<0.05 vs total BNP and proBNP in normal, †P<0.05 vs total BNP and proBNP in HF NYHA 1–2. Bar graph showing the total BNP, proBNP (C), proBNP/total BNP ratio (D) and NT-proBNP (E) levels in male and female in healthy subjects. Values are means ± SE. *P<0.05 vs male.
doi:10.1371/journal.pone.0053233.g006

and a fluorescent immunoenzyme assay to measure BNP and proBNP, we found that levels of BNP were slightly higher than those of proBNP in both healthy subjects and heart failure patients. The exact reason for the discrepancy in proBNP levels between the earlier study and the present one is unclear; however, the lower recovery caused by the need for extraction from plasma on a Sep-Pak C18 cartridge may have contributed to the lower proBNP levels in the earlier study [9,16]. Recent studies have shown that proBNP has much less ability to induce cGMP production in vascular smooth muscle and endothelial cells than BNP [7,18]. This suggests that increases in the levels of the low-activity proBNP in heart failure may contribute to the so-called "BNP paradox" [19]. That is, administration of exogenous recombinant human BNP to heart failure patients has a substantial clinical and hemodynamic impact, despite the presence of high levels of immunoreactive BNP in their plasma, as measured with commercially used BNP assays.

In the current study, we showed that total BNP and NT-proBNP increased with aging, which are consistent with the previous studies. In addition, the current study first showed that plasma proBNP level increased with aging. However, there were no statistical differences in NT-proBNP between 30~39 and 50~59, whereas there were significant differences in total and proBNP between 30~39 and 50~59, suggesting that total and proBNP are more sensitive than NT-proBNP. In addition, total and proBNP seemed to be well correlated with age ($r = 0.467$. 0.491, each) than NT-proBNP ($r = 0.376$). Thus, total BNP and proBNP may be better marker in discriminating the effect of age than NT-proBNP. Increased myocardial mass and/or reduction of renal clearance of natriuretic peptides with aging may be one of the possible reason for increased BNP and NT-BNP with aging; however, exact mechanism for it still remains unknown and further study is necessary to investigate the relationships between proBNP and aging.

We also analyzed the effects of gender on proBNP, total BNP, proBNP/total BNP ratio and NT-proBNP. Interestingly, in female higher total BNP and NT-proBNP and lower proBNP/total BNP ratio without changing of proBNP was observed. Calculated BNP (total BNP - proBNP) was also increased. This finding may be explained that increased proBNP production and higher processing rate. Further study is necessary to elucidate the mechanism of increased total BNP and NT-proBNP and lower proBNP/total BNP ratio without changing of proBNP in female.

In summary, we have developed rapid and precise immunochemiluminescent assay systems for routine determination of total BNP and proBNP levels in human plasma. Using these assay systems we showed that in addition to BNP, considerable amount of proBNP circulates in both healthy subjects and heart failure patients. The precise relation of the proBNP/total BNP ratio to heart failure remains unknown, as does whether the heart mainly secretes proBNP. Likewise, the effects of age, sex and renal function on proBNP levels remain unknown. We anticipate our new assays for the proBNP and total BNP will be helpful for addressing each of those issues.

## Acknowledgments

We thank Ms. Aoi Fujishima and Masako Matsubara for her excellent technical assistance and Ms.Yukari Kubo for her excellent secretarial work.

## Author Contributions

Gave useful comments and discussion: K. Kamgawa K. Nakao. Conceived and designed the experiments: TN HO NM KH. Performed the experiments: MN NO K. Nagata. Analyzed the data: YN HK CY K. Nakao. Contributed reagents/materials/analysis tools: TM YK K. Koichiro IM. Wrote the paper: TN HO.

## References

1. Maisel AS, Nakao K, Ponikowski P, Peacock WF, Yoshimura M, et al. (2011) Japanese-Western consensus meeting on biomarkers. Int Heart J. 52:253–65.
2. Jessup M, Abraham WT, Casey DE, Feldman AM, Francis GS, et al. (2009) ACCF/AHA Guidelines for the Diagnosis and Management of Heart Failure in Adults: a report of the American College of Cardiology Foundation/American Heart Association Task Force on Practice Guidelines: developed in collaboration with the International Society for Heart and Lung Transplantation. Circulation. 119:1977–2016.
3. Dickstein K, Cohen-Solal A, Filippatos G, McMurray JJ, Ponikowski P, et al. (2008) ESC Guidelines for the diagnosis and treatment of acute and chronic heart failure 2008: the Task Force for the Diagnosis and Treatment of Acute and Chronic Heart Failure 2008 of the European Society of Cardiology. Developed in collaboration with the Heart Failure Association of the ESC (HFA) and endorsed by the European Society of Intensive Care Medicine (ESICM). ESC Committee for Practice Guidelines (CPG). Eur Heart J. 29:2388–442.
4. Minamino N, Horio H, Nishikimi T (2006) Chapter 165. Natriuretic peptides in the cardiovascular system. In: Kastin AJ, editor. THE HANDBOOK OF BIOLOGICALLY ACTIVE PEPTIDES. 1st ed. Academic Press, pp. 1217–1225
5. Waldo SW, Beede J, Isakson S, Villard-Saussine S, Fareh J, et al. (2008) Pro-B-type natriuretic peptide levels in acute decompensated heart failure. J Am Coll Cardiol. 51:1874–82.
6. Nishikimi T, Minamino N, Ikeda M, Takeda Y, Tadokoro K, et al. (2010) Diversity of molecular forms of plasma brain natriuretic peptide in heart failure–different proBNP-108 to BNP-32 ratios in atrial and ventricular overload. Heart. 96:432–9.
7. Liang F, O'Rear J, Schellenberger U, Tai L, Lasecki M, et al. (2007) Evidence for functional heterogeneity of circulating B-type natriuretic peptide. J Am Coll Cardiol. 49:1071–8.
8. Nishikimi T, Minamino N, Horii K, Matsuoka H (2007) Do commercially available assay kits for B-type natriuretic peptide measure Pro-BNP1-108, as well as BNP1-32? Hypertension. 50:e163
9. Semenov AG, Seferian KR (2011) Biochemistry of the human B-type natriuretic peptide precursor and molecular aspects of its processing. Clin Chim Acta. 412:850–60
10. Tsuji T, Inouye K, Yamauchi A, Kono M, Igano K (2004) U.S. Patent 6, 677, 124 B2, pp 16, Shionogi Seiyaku Kabushiki Kaisha, Japan.
11. Seferian KR, Tamm NN, Semenov AG, Tolstaya AA, Koshkina EV, et al. (2008) Immunodetection of glycosylated NT-proBNP circulating in human blood. Clin Chem. 54:866–73.
12. Ishikawa E, Imagawa M, Hashida S, Yoshitake S, Hamaguchi Y, et al. (1983) Enzyme-labeling of antibodies and their fragments for enzyme immunoassay and immunohistochemical staining. J Immunoassay. 4:209–327.
13. Nishikimi T, Ikeda M, Takeda Y, Ishimitsu T, Shibasaki I, et al. (2012) The effect of glycosylation on plasma N-terminal proBNP-76 levels in patients with heart or renal failure. Heart. 98:152–61
14. Schellenberger U, O'Rear J, Guzzetta A, Jue RA, Protter AA, et al. (2006) The precursor to B-type natriuretic peptide is an O-linked glycoprotein. Arch Biochem Biophys. 451:160–6.
15. Nishikimi T, Kuwahara K, Nakao K. (2011) Current biochemistry, molecular biology, and clinical relevance of natriuretic peptides. J Cardiol. 57:131–40.
16. Seferian KR, Tamm NN, Semenov AG, Mukharyamova KS, Tolstaya AAet al. (2007) The brain natriuretic peptide (BNP) precursor is the major immunoreactive form of BNP in patients with heart failure. Clin Chem. 53:866–73.
17. Hammerer-Lercher A, Halfinger B, Sarg B, Mair J, Puschendorf B, et al. (2008) Analysis of circulating forms of proBNP and NT-proBNP in patients with severe heart failure. Clin Chem. 54:858–65.
18. Heublein DM, Huntley BK, Boerrigter G, Cataliotti A, Sandberg SM, et al. (2007) Immunoreactivity and guanosine 3′,5′-cyclic monophosphate activating actions of various molecular forms of human B-type natriuretic peptide. Hypertension. 49:1114–9.
19. Menon SG, Mills RM, Schellenberger U, Saqhir S, Protter AA (2009) Clinical implications of defective B-type natriuretic peptide. Clin Cardiol. 32:E36–41.

Genes to Cells

# Angiotensin II-induced cardiac hypertrophy and fibrosis are promoted in mice lacking *Fgf16*

**Emi Matsumoto[1], Sayaka Sasaki[1], Hideyuki Kinoshita[1], Takuya Kito[1], Hiroya Ohta[1], Morichika Konishi[1], Koichiro Kuwahara[2], Kazuwa Nakao[2] and Nobuyuki Itoh[1]***

[1]*Department of Genetic Biochemistry, Kyoto University Graduate School of Pharmaceutical Sciences, Sakyo, Kyoto 606-8501, Japan*
[2]*Department of Medicine and Clinical Science, Kyoto University Graduate School of Medicine, Sakyo, Kyoto 606-8507, Japan*

**Fibroblast growth factors (Fgfs) are pleiotropic proteins involved in development, repair and metabolism. *Fgf16* is predominantly expressed in the heart. However, as the heart function is essentially normal in *Fgf16* knockout mice, its role has remained unclear. To elucidate the pathophysiological role of Fgf16 in the heart, we examined angiotensin II-induced cardiac hypertrophy and fibrosis in *Fgf16* knockout mice. Angiotensin II-induced cardiac hypertrophy and fibrosis were significantly promoted by enhancing *Tgf-$\beta_1$* expression in *Fgf16* knockout mice. Unexpectedly, the response to cardiac remodeling was apparently opposite to that in *Fgf2* knockout mice. These results indicate that Fgf16 probably prevents cardiac remodeling, although Fgf2 promotes it. Cardiac *Fgf16* expression was induced after the induction of *Fgf2* expression by angiotensin II. In cultured cardiomyocytes, *Fgf16* expression was promoted by Fgf2. In addition, Fgf16 antagonized Fgf2-induced *Tgf-$\beta_1$* expression in cultured cardiomyocytes and noncardiomyocytes. These results suggest a possible mechanism whereby Fgf16 prevents angiotensin II-induced cardiac hypertrophy and fibrosis by antagonizing Fgf2. The present findings should provide new insights into the roles of Fgf signaling in cardiac remodeling.**

## Introduction

Fibroblast growth factors (Fgfs), proteins of ~150–300 amino acids, play diverse roles in development, repair and metabolism. The human/mouse Fgf family comprises twenty-two members (Itoh & Ornitz 2008, 2011). Most Fgfs mediate biological responses by binding to and activating Fgf receptors (Fgfrs) in a paracrine manner (Beenken & Mohammadi 2009; Itoh & Ornitz 2011). Among paracrine Fgfs, *Fgf16* is predominantly expressed in the heart. *Fgf16* expression is weakly detected in the embryonic heart and much more abundant at adult stages than embryonic stages. These findings indicate potential roles in the heart (Hotta *et al.* 2008; Lu *et al.* 2008a; Fon Tacer *et al.* 2010). Three lines of *Fgf16* knockout mice have been reported. Two of the lines are viable and fertile. Although the proliferation of embryonic cardiomyocytes temporarily decreases in our *Fgf16* knockout mice on a C57BL/6 background around embryonic day (E) 14.5, the heart function is essentially normal in *Fgf16* knockout mice (Hotta *et al.* 2008). The cardiac phenotype of the other *Fgf16* knockout mice on a 129/B6 background has not been reported (Hatch *et al.* 2009). In contrast, *Fgf16* knockout mice on a Black Swiss background died at around E11.5, indicating that Fgf16 is required for embryonic heart development in midgestation (Lu *et al.* 2008a). The phenotypes are potentially affected by genetic backgrounds (Lu *et al.* 2010).

As the heart function is essentially normal in *Fgf16* knockout mice, the role of Fgf16 in the heart remains unclear (Hotta *et al.* 2008). In hypertension, the heart responds to increased afterload by initiating adaptive remodeling processes including cardiac hypertrophy and fibrosis. Although *Fgf2* is broadly expressed in mice, hypertension-induced cardiac hypertrophy and fibrosis are less developed in *Fgf2* knockout mice, indicating that Fgf2 promotes them

*Communicated by*: Yo-ichi Nabeshima
**Correspondence*: itohnobu@pharm.kyoto-u.ac.jp


DOI: 10.1111/gtc.12055

(Virag *et al.* 2007; House *et al.* 2010). From these findings, we expected that Fgf16 also might play pathophysiological roles in the heart. The renin–angiotensin system is a key mediator of cardiac adaptations to hemodynamic overload. Angiotensin II induces hypertension and cardiac hypertrophy and fibrosis (Rosenkranz 2004). To elucidate the pathophysiological role of Fgf16 in the heart, we examined angiotensin II-induced cardiac hypertrophy and fibrosis in *Fgf16* knockout mice. Unexpectedly, possible adaptive remodeling processes were significantly promoted, indicating that the role of Fgf16 is apparently distinct from that of Fgf2. Here, we report a possible mechanism whereby Fgf16 prevents angiotensin II-induced cardiac hypertrophy and fibrosis.

## Results

### Compensatory cardiac response to angiotensin II is promoted in *Fgf16* knockout mice

We examined body and heart weights of wild-type and *Fgf16* knockout mice (Fig. 1A,B). Although body weight was essentially unchanged in the mice infused with angiotensin II for 14 days, heart weight was significantly increased. The *Fgf16* knockout mice had slightly but significantly heavier hearts than the wild-type mice. We also examined systolic blood pressure and echocardiographic parameters. Heart rate was essentially unchanged in both groups. However, systolic blood pressure tended to be increased in the wild-type mice and was significantly increased in the knockout mice (Fig. 1C,D). Interventricular septal thickness diastolic (IVSTd) and left ventricular end posterior wall dimension diastolic (LVPWd) were significantly increased in both groups. However, IVSTd and LVPWd in the knockout mice were similar to those in the wild-type mice (Fig. 1E–G). In contrast, left ventricular internal dimension diastolic (LVIDd) and left ventricle internal dimension systolic (LVIDs) were essentially unchanged in the wild-type mice, whereas they tended to be slightly increased in the knockout mice (Fig. 1E,H,I). Ejection fraction (EF) represents the volumetric fraction of blood pumped out of the heart with each heartbeat. Fractional shortening (FS) is used as an estimate of myocardial contractility. EF and FS were also essentially unchanged in the wild-type mice, but they tended to be slightly decreased in the knockout mice (Fig. 1J,K). These results suggest a possible compensatory cardiac response to angiotensin II is promoted in *Fgf16* knockout mice.

### Angiotensin II-induced cardiac hypertrophy and fibrosis are promoted in *Fgf16* knockout mice

Cardiac hypertrophy represents an adaptive process of the heart in response to work overload (Berk *et al.* 2007). Sections of heart stained with Masson's trichrome were examined by light microscopy (Fig. 2A). The size of cardiomyocytes was examined by determining the cells' cross-sectional area in LVPW (Fig. 2B,D). The size was significantly increased in both wild-type and *Fgf16* knockout mice infused with angiotensin II. However, it was significantly larger in the knockout mice. Cardiac remodeling is also associated with increased numbers of fibroblasts in the myocardium (Berk *et al.* 2007). Cardiac fibrosis is characterized by the increased deposition of extracellular matrix components and proliferation of interstitial fibroblasts. Extended fibrosis results in increased myocardial stiffness, causing ventricular dysfunction and ultimately heart failure (Weber & Brilla 1991). Interstitial fibrotic areas were stained with blue dye and quantitatively determined (Fig. 2C,E). The areas were markedly increased in both groups infused with angiotensin II. However, they were significantly larger in the knockout mice.

### Cardiac expression of genes related to cardiac remodeling is promoted in *Fgf16* knockout mice

Atrial natriuretic peptide (Anp) and brain natriuretic peptide (Bnp) are cardiac endocrine hormones/paracrine factors. *Anp* and *Bnp* expression levels are increased in the heart with cardiac hypertrophy and fibrosis (Nishikimi *et al.* 2006). β-Myosin heavy chain (βMhc) is one of the Mhc isoforms. *βMhc* expression levels are also increased in cardiac hypertrophy (Morkin 2000). We examined *Anp*, *Bnp* and *βMhc* expression in the heart by reverse transcription–quantitative polymerase chain reaction (RT-qPCR) (Fig. 3A–C). *Anp*, *Bnp* and *βMhc* expression levels were significantly or tended to be increased in both wild-type and *Fgf16* knockout mice infused with angiotensin II. Their levels tended to be higher in the knockout mice. Collagen type 1a (Col1a) is often defined as a component of extracellular matrices (Exposito *et al.* 2010). Connective tissue growth factor (Ctgf) is a matricellular protein that promotes angiogenesis. Periostin (Postn) is a secreted extracellular matrix protein belonging to the fasciclin family (Conway & Molkentin 2008). Matrix metallopeptidase 2 (Mmp2) plays a key role in matrix turnover (Stamenkovic 2003). Their expression is induced in

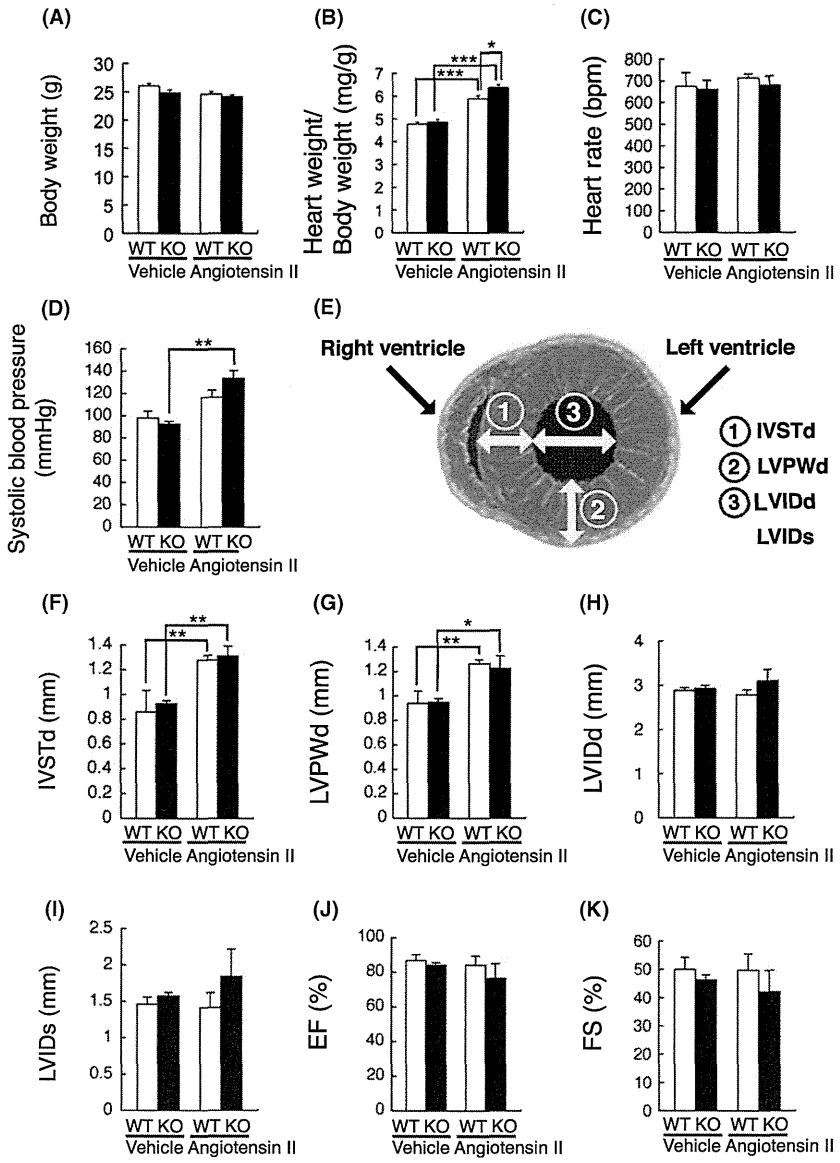


**Figure 1** Body and heart weights, systolic blood pressure and echocardiographic parameters. Body and heart weights (A, B), heart rate (C), systolic blood pressure (D), a schematic representation of cross-sectional cardiac anatomy (E), interventricular septal thickness diastolic (IVSTd) (F), left ventricular end posterior wall dimension diastolic (LVPWd) (G), left ventricular internal dimension diastolic (LVIDd) (H), left ventricle internal dimension systolic (LVIDs) (I), ejection fraction (EF) (J) and fractional shortening (FS) (K) were examined in both wild-type and *Fgf16* knockout mice infused with either vehicle or angiotensin II. Results are expressed as the mean ± SEM for mice infused with vehicle (wild type, $n$ = 3–11; *Fgf16* knockout, $n$ = 4–7) or angiotensin II (wild type, $n$ = 7–15; *Fgf16* knockout, $n$ = 5–14). Asterisks indicate statistical significance (*$P < 0.05$; **$P < 0.01$; ***$P < 0.001$).

hearts with cardiac fibrosis (Bergman *et al.* 2007; Nishida *et al.* 2008; Leask 2010). Their cardiac expression levels were significantly or tended to be increased in both groups infused with angiotensin II (Fig. 3D–G). Their levels were significantly or tended to be higher in the knockout mice. These results support those of the histochemical analysis.

Transforming growth factor-$\beta_1$ (Tgf-$\beta_1$) is also a key mediator of cardiac adaptations to hemodynamic overload and thus critically involved in the pathogenesis of cardiac hypertrophy and fibrosis. Tgf-$\beta_1$ acts downstream of angiotensin II and promotes angiotensin II-induced cardiac hypertrophy and fibrosis (Rosenkranz 2004). Cardiac *Tgf-$\beta_1$* expression levels

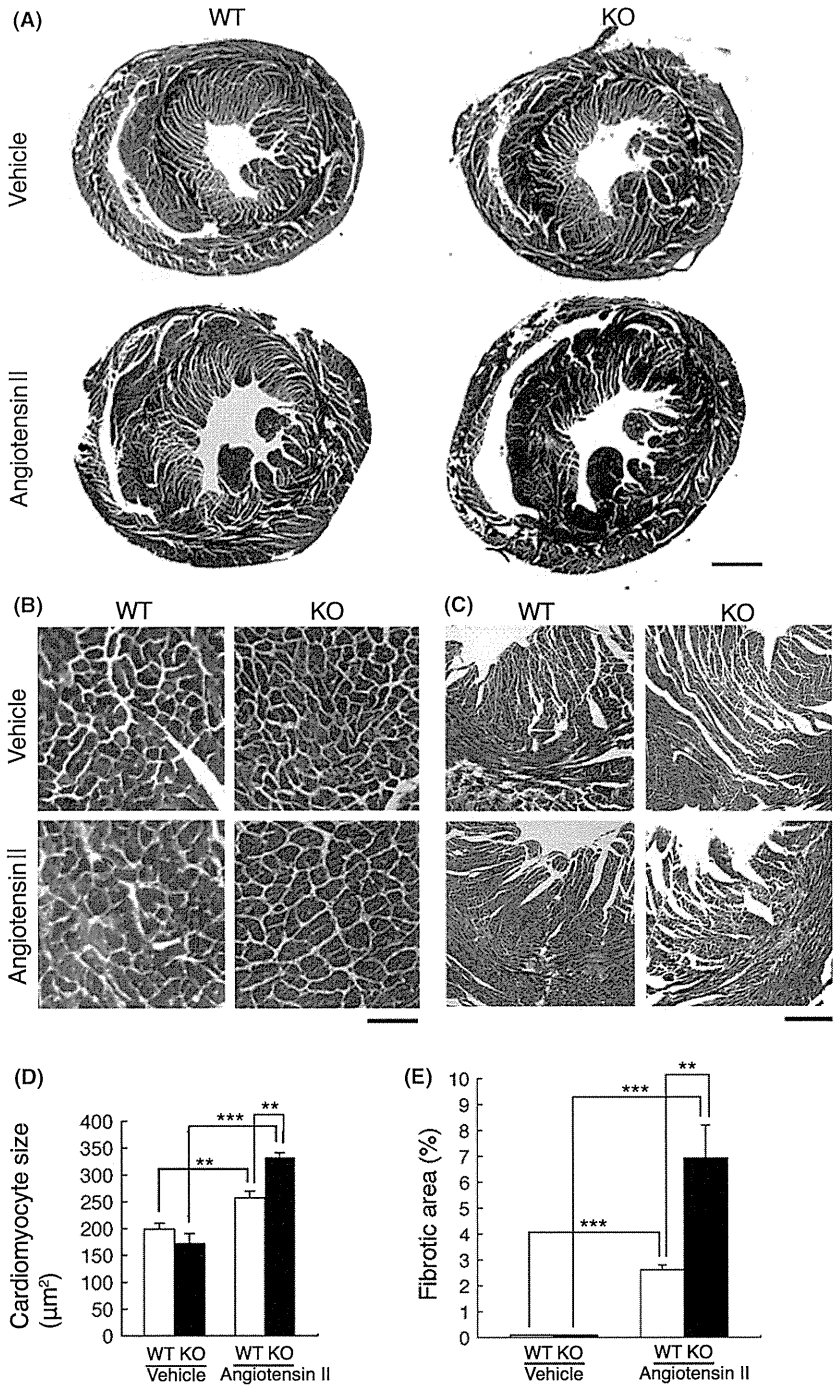


**Figure 2** Cardiac hypertrophy and fibrosis. Sections of the heart were stained with Masson's trichrome (A). The size of cardiomyocytes in the section of left ventricular end posterior wall (LVPW) was determined from the cells' cross-sectional area (B, D). Blue-stained interstitial fibrotic areas in the sections were quantitatively determined (C, E). Results are expressed as the mean ± SEM for mice infused with vehicle (wild type, $n$ = 5–7; *Fgf16* knockout, $n$ = 4–6) or angiotensin II (wild type, $n$ = 6–14; *Fgf16* knockout, $n$ = 4–12). Asterisks indicate statistical significance (**$P < 0.01$; ***$P < 0.001$). Scale bars = 1 μm (A), 50 μm (B) and 300 μm (C).

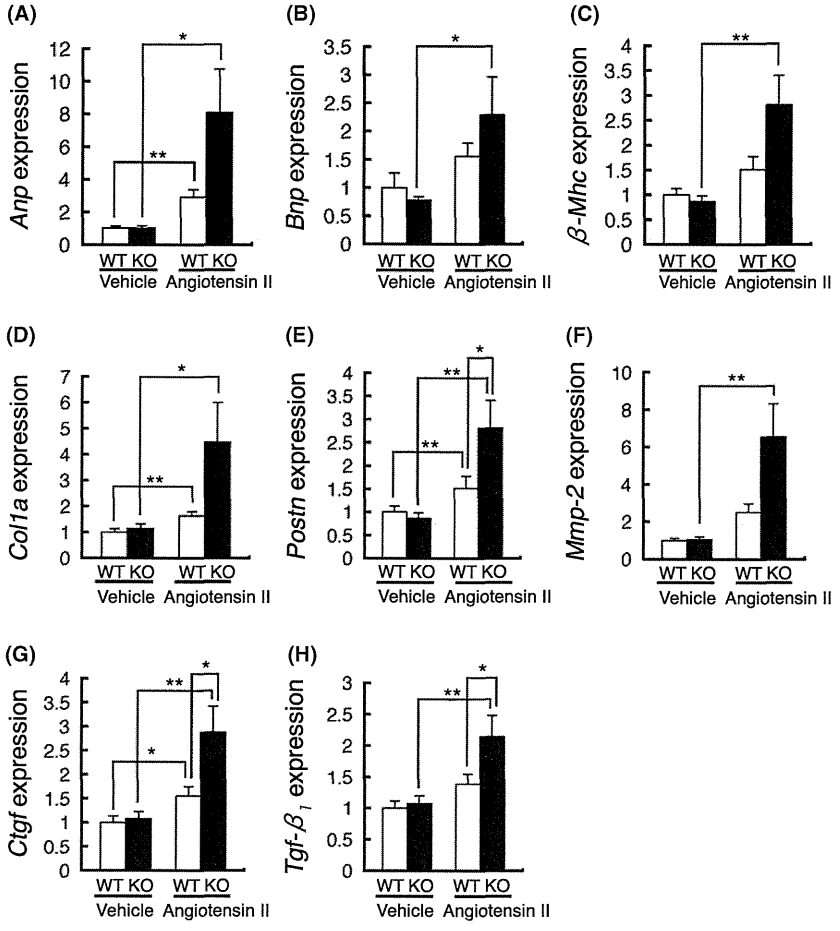


**Figure 3** Cardiac expression of genes related to cardiac hypertrophy and/or fibrosis. Cardiac expression of their genes (A–H) was examined by RT-qPCR. Results are expressed as the mean ± SEM for mice infused with vehicle (wild type, $n = 10$; *Fgf16* knockout, $n = 7$) or angiotensin II (wild type, $n = 16$; *Fgf16* knockout, $n = 15$). Asterisks indicate statistical significance ($\star P < 0.05$; $\star\star P < 0.01$).

were increased in both mice infused with angiotensin II (Fig. 3H). In addition, its levels were significantly higher in the knockout mice.

### Fgf16 antagonizes Fgf2-induced *Tgf-β1* expression in cultured cardiomyocytes and noncardiomyocytes

Lu *et al.* reported that Fgf2 showed significant proliferative activity in cultured neonatal rat cardiomyocytes, but Fgf16 did not. However, Fgf16 antagonized the activity of Fgf2 (Lu *et al.* 2008b). Cultured neonatal rat cardiomyocytes and noncardiomyocytes have been well-established (Nakagawa *et al.* 1995), but mouse cells not. We also examined the effects of Fgf16 and Fgf2 on *Tgf-β1* expression in cultured neonatal rat cardiomyocytes and noncardiomyocytes (Fig. 4A,B). Although Fgf2 significantly induced *Tgf-β1* expression in both cells, Fgf16 did not. However, Fgf16 repressed Fgf2-induced *Tgf-β1* expression, indicating that Fgf16 antagonizes Fgf2-induced *Tgf-β1* expression. These results are essentially consistent with the results by Lu *et al.* (Lu *et al.* 2008b).

### Cardiac Fgf16 and Fgf2 expression levels are increased by angiotensin II infusion

We examined cardiac *Fgf16* and *Fgf2* expression in the mice infused with angiotensin II for 1–14 days (Fig. 4C,D). Both *Fgf16* and *Fgf2* expression levels were significantly increased by angiotensin II infusion. *Fgf2* expression levels were maximally increased at 2 days and thereafter gradually decreased. However, *Fgf16* expression levels were maximally

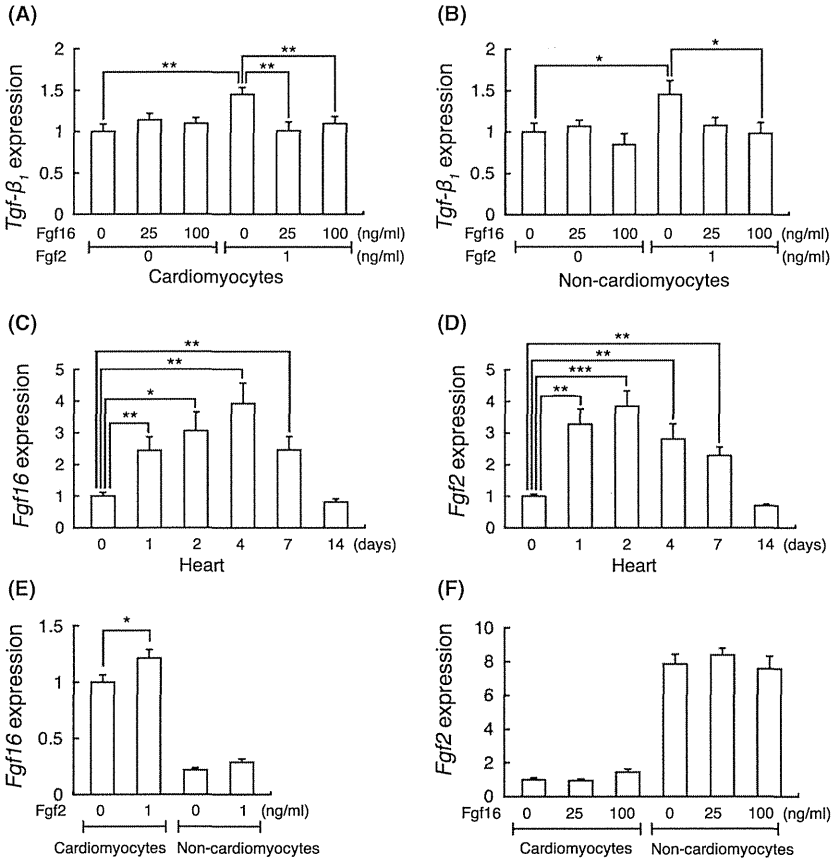


**Figure 4** Effects of Fgf16 and Fgf2 in cultured cardiomyocytes and noncardiomyocytes and *Fgf16* and *Fgf2* expression in the heart. The effects of Fgf16 and Fgf2 on *Tgf-β1* expression in cultured cardiomyocytes and noncardiomyocytes were examined by RT-qPCR (A, B). Cardiac *Fgf16* and *Fgf2* expression in mice infused with angiotensin II for 1–14 days was examined by RT-qPCR (C, D). The effect of Fgf2 on *Fgf16* expression in cultured cardiomyocytes and noncardiomyocytes were examined by RT-qPCR (E). The effect of Fgf16 on *Fgf12* expression in cultured cardiomyocytes and noncardiomyocytes was examined by RT-qPCR (F). Results are expressed as the mean ± SEM for mice infused with angiotensin II ($n$ = 5–15) and the cultured cells ($n$ = 11–14). Asterisks indicate statistical significance (*$P < 0.05$; **$P < 0.01$; ***$P < 0.001$).

increased at 4 days and thereafter gradually decreased, indicating that *Fgf16* expression was induced after the induction of *Fgf2* expression in the heart.

### Fgf2 stimulates Fgf16 expression in cultured neonatal rat cardiomyocytes

We examined *Fgf16* and *Fgf2* expression in cultured neonatal rat cardiomyocytes and noncardiomyocytes. *Fgf16* was more abundantly expressed in cardiomyocytes than noncardiomyocytes (Fig. 4E). In contrast, Fgf2 was more abundantly expressed in noncardiomyocytes than cardiomyocytes (Fig. 4F). Low *Fgf16* and *Fgf2* expression levels in cultured noncardiomyocytes and cardiomyocytes might reflect the possibility of cross-contamination of one cell versus the other, respectively. We also examined the effect of Fgf2 on *Fgf16* expression in both cells. Fgf2 stimulated *Fgf16* expression in cultured cardiomyocytes but not noncardiomyocytes (Fig. 4E). In addition, we also examined the effect of Fgf16 on *Fgf2* expression in both cells. However, Fgf16 did not affect *Fgf2* expression in both cells (Fig. 4F).

## Discussion

Fgf16 acts as a local paracrine signaling molecule. *Fgf16* expression levels are much more abundant at adult stages than at embryonic stages, indicating potential roles of Fgf16 in the heart at adult stages (Hotta *et al.* 2008; Lu *et al.* 2008a). However, as heart function examined by echocardiography is essentially

normal in *Fgf16* knockout mice at adult stages (Hotta *et al.* 2008), the roles of Fgf16 in the adult heart remain unclear.

The renin–angiotensin system is a key mediator of cardiac adaptations to hemodynamic overload. In hypertension, the heart responds to increased afterload by initiating adaptive remodeling processes, including cardiac hypertrophy and fibrosis (Rosenkranz 2004). Although these structural alterations represent the heart's efforts to maintain systolic function, they are deleterious over time and ultimately result in progressive heart failure. Angiotensin II induces cardiac hypertrophy and fibrosis (Rosenkranz 2004). To examine pathophysiological roles of Fgf16 in the adult heart, we examined the heart of *Fgf16* knockout mice injected with angiotensin II.

### Fgf16 contributes to a myocardial environment that protects against hypertrophy and fibrosis

Systolic blood pressure tends to be increased in *Fgf16* knockout mice with angiotensin II infusion. In addition, dilated cardiomyopathy is also slightly induced in *Fgf16* knockout mice with angiotensin II infusion. Compensatory cardiac failure response to angiotensin II is promoted in *Fgf16* knockout mice. Histological analysis indicates that angiotensin II-induced cardiac hypertrophy and fibrosis are significantly promoted in *Fgf16* knockout mice. Increased expression levels of marker genes for cardiac hypertrophy and/or fibrosis also support promoted angiotensin II-induced cardiac hypertrophy and fibrosis in *Fgf16* knockout mice. These observations suggest that endogenous Fgf16 contributes to a myocardial environment that protects against hypertrophy and fibrosis, at least when the stress is induced by Angiotensin II.

### Tgf-$\beta_1$ may promote angiotensin II-induced cardiac remodeling in *Fgf16* knockout mice

Tgf-$\beta_1$ critically involved in the pathogenesis of cardiac hypertrophy and fibrosis. Angiotensin II induces cardiac hypertrophy and fibrosis by up-regulation of *Tgf-$\beta_1$* expression via the angiotensin II type 1 receptor in cardiac myocytes and fibroblasts. Induction of *Tgf-$\beta_1$* is absolutely required for angiotensin II-induced cardiac hypertrophy and fibrosis in mice, indicating that Tgf-$\beta_1$ acts downstream of angiotensin II (Rosenkranz 2004). Cardiac *Tgf-$\beta_1$* expression levels in *Fgf16* knockout mice with angiotensin II infusion are significantly higher than those in wild-type mice. These observations are consistent with a requirement for Tgf-β1 signaling in the promotion of angiotensin II-induced cardiac hypertrophy and fibrosis in *Fgf16* knockout mice.

### Different responses to cardiac hypertrophy and fibrosis in *Fgf16* and *Fgf2* knockout mice

Although most *Fgf* genes have been disrupted by gene targeting in mice, cardiac phenotypes at adult stages have been shown in only *Fgf2* knockout mice (Itoh & Ornitz 2011). Cardiac hypertrophy and fibrosis were less developed in *Fgf2* knockout mice with myocardial infarcts (Virag *et al.* 2007). Furthermore, isoproterenol-induced cardiac hypertrophy was protected in *Fgf2* knockout mice (House *et al.* 2010). The cardiac phenotypes of *Fgf2* knockout mice are apparently opposite to that of *Fgf16* knockout mice reported here.

### Possible mechanism of Fgf16 action in cardiac hypertrophy and fibrosis

*Fgf16* is expressed mainly in cardiomyocytes. Fgf16 is efficiently secreted and acts as a paracrine signaling molecule (Miyake *et al.* 1998; Itoh & Ornitz 2011). In contrast, Fgf2 is mainly expressed in noncardiomyocytes. The biochemical properties of Fgf2 are also distinct from those of Fgf16. Fgf2, which has not a secretory signal sequence, is not a typical secretory protein. Fgf2 might be released from damaged cells or by an exocytotic mechanism that is independent of the endoplasmic reticulum–Golgi pathway (Nickel 2010). Fgf2, which is stored in these cells, is released in response to a hemodynamic stress (Clark *et al.* 1995; Kaye *et al.* 1996).

The phenotype of *Fgf16* knockout mice indicates that Fgf16 probably prevents angiotensin II-induced cardiac hypertrophy and fibrosis by repressing *Tgf-$\beta_1$* expression in mice. The role of Fgf16 is apparently opposite to that of Fgf2, which promotes them, indicating that the role of Fgf16 in cardiac remodeling is clearly distinct from that of Fgf2. Although Fgf16 does not induce *Tgf-$\beta_1$* expression in cultured cardiomyocytes and noncardiomyocytes, Fgf16 antagonizes Fgf2-induced *Tgf-$\beta_1$* expression in both cells. *Fgf16* expression is induced after the induction of *Fgf2* expression in the heart. In cultured cardiomyocytes, *Fgf16* expression is induced by Fgf2. In contrast, *Fgf2* expression is not affected by Fgf16 in cultured cardiomyocytes and noncardiomyocytes. There are seven major Fgfr proteins (Fgfrs 1b, 1c, 2b, 2c, 3b, 3c and 4) with differing ligand-binding specificity (Beenken

& Mohammadi 2009; Itoh & Ornitz 2011). Among these *Fgfr*s, the heart predominantly expresses *Fgfr1c* (Fon Tacer *et al.* 2010). Fgf16 competes with Fgf2 for the binding site for Fgfr1c (Lu *et al.* 2008b). These results suggest a possible mechanism whereby Fgf16 probably prevents angiotensin II-induced cardiac hypertrophy and fibrosis by competing with Fgf2 for the binding site for Fgfr1c.

## Experimental procedures

### Animal experiments

Wild-type and *Fgf16* knockout mice on a C57BL/6 background were maintained in a light-controlled room and allowed free access to a normal diet (Hotta *et al.* 2008). Only male mice were used for experiments. Our ethics committee specifically approved this study. All animal studies were conducted in accordance with principles by the Animal Research Committee of Kyoto University Pharmaceutical Sciences, based on International Guiding Principles for Biomedical Research Involving Animals.

### Angiotensin II infusion

Mice at 10 weeks of age were subcutaneously implanted with an osmotic minipump (Alzet model 2002, Alza Corp) to continuously infuse angiotensin II in 10 mM acetic acid at a dose of 1.44 μg/g per day or an identical volume of 10 mM acetic acid as vehicle.

### Echocardiography

Mice at 12 weeks of age infused for 14 days were examined by conscious echocardiography. During the echocardiography, the animals were restrained by grasping the skin on the back of the neck and wrapping the tail (Xu *et al.* 2007). Heart rate, LVIDd, LVIDs, FS, EF, IVSTd and LVIDs were calculated using an echocardiographic system (Toshiba Power Vision 8000) equipped with a 12-MHz imaging transducer (Nakanishi *et al.* 2007). Systolic blood pressure was measured in conscious mice at 12 weeks of age using a noninvasive computerized tail-cuff method (Kuwahara *et al.* 2010).

### Histological analysis

The heart was fixed overnight in 10% formaldehyde, dehydrated, embedded in paraffin and sectioned at 6 μm. Sections stained with Masson's trichrome were examined by light microscopy. Images of the heart sections were captured. Cardiomyocyte sizes were quantitatively determined with Image J software. Blue-stained interstitial fibrotic areas were also quantitatively determined with Image J software.

### Expression analysis by RT-qPCR

cDNA was synthesized from RNA extracted from the heart. The cDNA was amplified by qPCR (Hotta *et al.* 2008), using the following primers: mouse/rat *18S rRNA* (sense primer, 5′-CCA ACG TCT GCC CTA TCA ACT T-3′; antisense primer, 5′-CCG GAA TCG AAC C CT GAT T-3′), mouse *Anp* (sense primer, 5′-TTC TTC CTC GTC TTG GCC TTT-3′; antisense primer, 5′-GAC CTC ATC TTC TAC CGG CAT CT-3′), mouse *Bnp* (sense primer, 5′-CAC CGC TGG GAG GTC ACT-3′; antisense primer, 5′-GTG AGG CCT TGG TCC TTC AAG GTC ACT-3′), mouse *βMhc* (sense primer, 5′-ATG TGC CGG ACC TTG GAA-3′; antisense primer, 5′-CCT CGG GTT AGC TGA GAG ATC A-3′), mouse *Col1a* (sense primer, 5′-CGA AGG CAA CAG TCG CTT CA-3′; antisense primer, 5′-GGT CTT GGT GGT TTT GTA TTC GA-3′), mouse *Ctgf* (sense primer, 5′-AGC AGC TGG GAG AAC TGT GT-3′; antisense primer, 5′-GCT GCT TTG GAA GGA CTC AC-3′), mouse *Postn* (sense primer, 5′-AAC CAA GGA CCT GAA ACA CG-3′; antisense primer, 5′-TGT GTC AGG ACA CGG TCA AT-3′), mouse *Mmp2* (sense primer, 5′-TTT GCT CGG GCC TTA AAA GTA T-3′; antisense primer, 5′-CCA TCA AAT GGG TAT CCA TCT C-3′), mouse *Tgf-β1* (sense primer, 5′-CTG CGC TTG CAG AGA TTA AA-3′; antisense primer, 5′-GAA AGC CCT GTA TTC CGT CT-3′), rat *Tgf-β1* (sense primer, 5′-CTG CGC CTG CAG AGA TTC AA-3′; antisense primer, 5′-GAA AGC CCT GTA TTC CGT CT-3′), moue/rat *Fgf16* (sense primer, 5′-CTG ATC AGC ATC AGG GGA GT-3′; antisense primer, 5′-AGG TGG AGG CAT AGG TGT TG-3′), moue *Fgf2* (sense primer, 5′-AGC GAC CCA CAC GTC AAA CT-3′; antisense primer, 5′-CGT CCA TCT TCC TTC ATA GCA AG-3′) and rat *Fgf2* (sense primer, 5′-GAC GGC TGC TGG CTT CTA AGT-3′; antisense primer, 5′-TTT CCG TGA CCG GTA AGT GTT-3′). *18S* rRNA levels were used as an internal control.

### Cell culture

Cardiomyocytes and noncardiomyocytes were prepared from apical halves of cardiac ventricles from Wistar rats at 1 or 2 days of age (Nakagawa *et al.* 1995) and plated at a density of $3.5 \times 10^4$ cells/cm$^2$ in gelatin-coated 24-well culture dishes (Becton Dickinson) in Dulbecco's modified Eagle's medium (DMEM) supplemented with 10% fetal bovine serum, 100 U/ml penicillin G and 100 μg/ml streptomycin. After a 40-h incubation, the cells were maintained in serum-free DMEM for 10 h. After a preconditioning period, the cultures were incubated in serum-free DMEM containing 1 mg/ml BSA with 1 ng/ml recombinant Fgf2 and/or 25 or 100 ng/ml recombinant Fgf16 (Danilenko *et al.* 1999) for 40 h. cDNA was synthesized from RNA extracted from cultured cardiomyocytes. *Tgf-β1*, *Fgf2* and *Fgf16* expression levels were examined by qPCR as described above.

### Statistical analysis

Results are expressed as the mean ± standard error of measurement (SEM). The statistical significance of differences in mean values was assessed with Student's *t*-test.

## Acknowledgements

This work was supported by a Grant-in-aid for Scientific Research from the Ministry of Education, Science, Culture and Sports of Japan and the Takeda Science Foundation, Japan.

## References

Beenken, A. & Mohammadi, M. (2009) The FGF family: biology, pathophysiology and therapy. *Nat. Rev. Drug Discov.* **8**, 235–253.

Bergman, M.R., Teerlink, J.R., Mahimkar, R., Li, L., Zhu, B.Q., Nguyen, A., Dahi, S., Karliner, J.S. & Lovett, D.H. (2007) Cardiac matrix metalloproteinase-2 expression independently induces marked ventricular remodeling and systolic dysfunction. *Am. J. Physiol. Heart Circ. Physiol.* **292**, H1847–H1860.

Berk, B.C., Fujiwara, K. & Lehoux, S. (2007) ECM remodeling in hypertensive heart disease. *J. Clin. Invest.* **117**, 568–575.

Clark, M.S., Caldwell, R.W., Chiao, H., Miyake, K. & McNeil, P.L. (1995) Contraction-induced cell wounding and release of fibroblast growth factor in heart. *Circ. Res.* **76**, 927–934.

Conway, S.J. & Molkentin, J.D. (2008) Periostin as a heterofunctional regulator of cardiac development and disease. *Curr. Genomics* **9**, 548–555.

Danilenko, D.M., Montestruque, S., Philo, J.S., *et al.* (1999) Recombinant rat fibroblast growth factor-16: structure and biological activity. *Arch. Biochem. Biophys.* **361**, 34–46.

Exposito, J.Y., Valcourt, U., Cluzel, C. & Lethias, C. (2010) The fibrillar collagen family. *Int. J. Mol. Sci.* **11**, 407–426.

Fon Tacer, K., Bookout, A.L., Ding, X., Kurosu, H., John, G.B., Wang, L., Goetz, R., Mohammadi, M., Kuro-o, M., Mangelsdorf, D.J. & Kliewer, S.A. (2010) Research resource: comprehensive expression atlas of the fibroblast growth factor system in adult mouse. *Mol. Endocrinol.* **24**, 2050–2064.

Hatch, E.P., Urness, L.D. & Mansour, S.L. (2009) Fgf16 (IRESCre) mice: a tool to inactivate genes expressed in inner ear cristae and spiral prominence epithelium. *Dev. Dyn.* **238**, 358–366.

Hotta, Y., Sasaki, S., Konishi, M., Kinoshita, H., Kuwahara, K., Nakao, K. & Itoh, N. (2008) Fgf16 is required for cardiomyocyte proliferation in the mouse embryonic heart. *Dev. Dyn.* **237**, 2947–2954.

House, S.L., House, B.E., Glascock, B., Kimball, T., Nusayr, E., Schultz, J.E. & Doetschman, T. (2010) Fibroblast Growth Factor 2 Mediates Isoproterenol-induced Cardiac Hypertrophy through Activation of the Extracellular Regulated Kinase. *Mol. Cell. Pharmacol.* **2**, 143–154.

Itoh, N. & Ornitz, D.M. (2008) Functional evolutionary history of the mouse Fgf gene family. *Dev. Dyn.* **237**, 18–27.

Itoh, N. & Ornitz, D.M. (2011) Fibroblast growth factors: from molecular evolution to roles in development, metabolism and disease. *J. Biochem.* **149**, 121–130.

Kaye, D., Pimental, D., Prasad, S., Mäki, T., Berger, H.J., McNeil, P.L., Smith, T.W. & Kelly, R.A. (1996) Role of transiently altered sarcolemmal membrane permeability and basic fibroblast growth factor release in the hypertrophic response of adult rat ventricular myocytes to increased mechanical activity in vitro. *J. Clin. Invest.* **97**, 281–291.

Kuwahara, K., Kinoshita, H., Kuwabara, Y., Nakagawa, Y., Usami, S., Minami, T., Yamada, Y., Fujiwara, M. & Nakao, K. (2010) Myocardin-related transcription factor A is a common mediator of mechanical stress- and neurohumoral stimulation-induced cardiac hypertrophic signaling leading to activation of brain natriuretic peptide gene expression. *Mol. Cell. Biol.* **30**, 4134–4148.

Leask, A. (2010) Potential therapeutic targets for cardiac fibrosis: TGFbeta, angiotensin, endothelin, CCN2, and PDGF, partners in fibroblast activation. *Circ. Res.* **106**, 1675–1680.

Lu, S.Y., Jin, Y., Li, X., Sheppard, P., Bock, M.E., Sheikh, F., Duckworth, M.L. & Cattini, P.A. (2010) Embryonic survival and severity of cardiac and craniofacial defects are affected by genetic background in fibroblast growth factor-16 null mice. *DNA Cell Biol.* **29**, 407–415.

Lu, S.Y., Sheikh, F., Sheppard, P.C., Fresnoza, A., Duckworth, M.L., Detillieux, K.A. & Cattini, P.A. (2008a) FGF-16 is required for embryonic heart development. *Biochem. Biophys. Res. Commun.* **373**, 270–274.

Lu, S.Y., Sontag, D.P., Detillieux, K.A. & Cattini, P.A. (2008b) FGF-16 is released from neonatal cardiac myocytes and alters growth-related signaling: a possible role in postnatal development. *Am. J. Physiol. Cell Physiol.* **294**, C1242–C1249.

Miyake, A., Konishi, M., Martin, F.H., Hernday, N.A., Ozaki, K., Yamamoto, S., Mikami, T., Arakawa, T. & Itoh, N. (1998) Structure and expression of a novel member, FGF-16, on the fibroblast growth factor family. *Biochem. Biophys. Res. Commun.* **243**, 148–152.

Morkin, E. (2000) Control of cardiac myosin heavy chain gene expression. *Microsc. Res. Tech.* **50**, 522–531.

Nakagawa, O., Ogawa, Y., Itoh, H., Suga, S., Komatsu, Y., Kishimoto, I., Nishino, K., Yoshimasa, T. & Nakao, K. (1995) Rapid transcriptional activation and early mRNA turnover of brain natriuretic peptide in cardiocyte hypertrophy. *J. Clin. Invest.* **96**, 1280–1287.

Nakanishi, M., Harada, M., Kishimoto, I., Kuwahara, K., Kawakami, R., Nakagawa, Y., Yasuno, S., Usami, S., Kinoshita, H., Adachi, Y., Fukamizu, A., Saito, Y. & Nakao, K. (2007) Genetic disruption of angiotensin II type 1a receptor improves long-term survival of mice with chronic severe aortic regurgitation. *Circ. J.* **71**, 1310–1316.

Nickel, W. (2010) Pathways of unconventional protein secretion. *Curr. Opin. Biotechnol.* **21**, 621–626.

Nishida, M., Sato, Y., Uemura, A., Narita, Y., Tozaki-Saitoh, H., Nakaya, M., Ide, T., Suzuki, K., Inoue, K., Nagao, T.